Multimodal Brain Mapping of General Intelligence

Nina Chung Mathiesen

Master's Thesis at the Department of Psychology

UNIVERSITY OF OSLO

October 2015

2015

Multimodal Brain Mapping of General Intelligence

Nina Chung Mathiesen

http://www.duo.uio.no/

Trykk: Reprosentralen, Universitetet i Oslo

Summary

Name of author: Nina Chung Mathiesen

Title of thesis: *Multimodal Brain Mapping of General Intelligence*

Main supervisor: Lars Tjelta Westlye

Co-supervisor: Nhat Trung Doan

General intelligence (*g*) is the proposed psychometric structure explaining the positive manifold between different cognitive tests. Currently, there is no consensus as to the cognitive underpinnings of *g*. However, the *mutualism model* suggests that there is no singular neurobiological or cognitive structure underlying *g*; but that *g* is caused by correlated yet distinct cognitive processes. From a neurobiological standpoint, various indices of grey and white matter are assumed to be associated with *g*. Nevertheless, there is little research examining whether these amount to separate underlying structures.

A recently developed technique for data fusion allowed us to assess the multimodal neurobiological underpinnings for *g*. Linked ICA was used to fuse indices of grey (VBM, cortical thickness, surface area) and white matter (DTI measures fractional anisotropy, mean diffusivity, mode of anisotropy) from 266 healthy participants aged 17-46. This was decomposed into fifty multimodal components of structural variance in the neuroimaging data across participants. To the extent that *g* was associated with different underlying structures, we expected these to be represented in different components. The subject weights on the different components were associated with the participants' *g* scores. *g* was derived using Principal Axis Factoring on 16 cognitive tests. Nominally significant components were kept for further analysis. Their structure is described in detail, and discussed in terms of previous research and putative function.

We hypothesized that *g* was not unitary at the neurobiological level, but would be associated with several components. We observed a brain-wide global white matter microstructure component, a component driven by higher integrity in major white matter tracts, and a component related to greater surface area in circumscribed cortical regions. All 34 components explained a large portion of variance in *g*, but no single component explained more than 3% of variance on its own. This strongly suggests that *g* has multiple structural underpinnings.

This study was an independent research project, and used existing data from the Thematically Organized Psychosis (TOP) Project. The idea for the project was conceived by the author, although help was received in implementing Linked ICA.

Abstract

g is the positive manifold between cognitive tests, and appears as a singular psychometric property. Although *g* is associated with different white and grey matter structures, it is not known whether these represent different neurobiological underpinnings to *g*. Thus, the structural underpinnings of *g* are not clear. This study takes a novel approach to fuse grey and white matter neuroimaging biomarkers, and to derive multimodal components reflecting independent variance. Linked Independent Component Analysis (Linked ICA) was performed on 226 healthy participants, and included the grey matter modalities cortical surface area, cortical thickness, voxel-based morphometry (VBM); and diffusion tensor imaging (DTI) based modalities fractional anisotropy, mean diffusivity, and the mode of anisotropy. Fifty independent components were derived, of which three were significantly associated with *g*. The first component was characterised by global white matter microstructure. The second component showed higher white matter integrity in major association, projection, and commissural tracts; with a concomitant decrease in cortical volume and thickness. The third component was characterised by greater cortical surface area in circumscribed frontal, temporal, parietal, and occipital regions; and white matter microstructure changes in commissural tracts. Together all components explained 18.4% of variance in *g*, but no single component explained more than 3%. This strongly suggests that *g* has multiple neurobiological underpinnings. Thus, the common variance feeding into psychometric *g* does not reflect a unitary *g* at the neurobiological level.

Acknowledgements

I would like to thank my supervisor Lars Tjelta Westlye for his guidance, patience and generosity during all phases of the project. You have taught me valuable lessons in the art of thinking clearly. Furthermore I would like to thank my co-supervisor Nhat Trung Doan, for helping me with the MATLAB aspect of Linked ICA. I value our methodological discussions very much. I would also like to thank my associates at the TOP Project for giving me access to their data and including me in their activities. In particular I would like to thank Siren Tønnesen for allowing me to use her DTI-data and Martina Jonette Lund for teaching me the basics of LINUX. A special thanks goes to people who have read my drafts at various stages of the writing process: Daniel Quintana, Røskva Bjørgfinsdóttir, Johanna Katarina Blomster, Andrea Duarte Silva, Rabiya Anjem, Mathias Ormestad Frendem, Lily Sandstrom, and Karl Olaf Mathiesen.

Anyone who has written an academic paper knows that it can be a very challenging process, both academically and personally. Therefore, I cannot thank enough the family and friends who have supported me through this process. Without everyone's support, conversation, and encouragement I could not have written this thesis. Any mistakes are entirely my own.

Table of Contents

Multimodal Brain Mapping of General Intelligence

People who are good at one thing tend to be good at other things as well. Behind this everyday observation is one of the best documented phenomena in modern psychology. Within psychometrics, it has been universally observed that performance on nearly all mental tests correlate with each other (Carroll, 1993; Jensen, 1998; Spearman, 1927). This so-called "positive manifold" has given rise to the widely-accepted theory of general intelligence (*g* or *g* factor), which postulates that a single psychometric factor explains the shared variance between tests of mental ability (Spearman, 1904, 1927).

Still, neither the cognitive nor neurobiological underpinnings of *g* are completely understood (for reviews, see Colom, Karama, Jung, & Haier, 2010; Deary, Penke, & Johnson, 2010; Nisbett et al., 2012). Psychometrically, there is only one *g*. However, it has been suggested that *g* may be comprised of multiple cognitive components rather than a single unitary component (Van Der Maas et al., 2006). Similarly, various indices of grey and white matter are associated with *g* (e.g. Barbey et al., 2012; Jung & Haier, 2007; Narr et al., 2007; Penke et al., 2012; Schmithorst, Wilke, Dardzinski, & Holland, 2005). It is not clear whether grey and white matter belong to the same underlying structure for *g* or not. Nonetheless, neurobiological structures are hypothesized to have multimodal underpinnings (i.e., are made up of different morphometric indices; Zatorre, Fields, & Johansen-Berg, 2012). To our knowledge, no studies have hitherto mapped the multimodal structures underlying *g* on a voxel-level. In other words, the number of neurobiological structures underlying of *g*, as well as their multimodal composition, are not known.

We hypothesised that *g* is not unitary on a neurobiological level, and that there are several underlying structures associated with *g*. To test this, we employed a novel method, Linked Independent Component Analysis (linked ICA; Groves, Beckmann, Smith, & Woolrich, 2011), to decompose inter-subject variability into multimodal components of grey and white matter variance. The subjects' weighting on to each component was then correlated with the subjects' calculated *g.* As given by the name, Linked ICA yields statistically independent components, which represent independent neurobiological structures. Thus we were able to map the number of structures associated with *g*, as well as their multimodal makeup. Below we will review the cognitive models associated with *g*. We will then review the relevant structural neuroimaging literature, before explaining the utility of Linked ICA in investigating the neurobiology of *g*.

Intelligence and *g*

Intelligence is notoriously hard to define in narrow terms, and appears to encompass a broad range of abilities. One definition of intelligence with wide consensus is "a very general capability that, among other things, involves the ability to reason, plan, solve problems, think abstractly, comprehend complex ideas, learn quickly, and learn from experience" (Gottfredson, 1997, p. 13). Yet despite the fact that intelligence is associated with a wide range of behaviours, it exists as a strong and unitary folk psychological concept. We tend to make assessments of others as being more or less intelligent. Perhaps it is therefore not surprising that intelligence has a strong probabilistic relationship with a variety of real-world outcomes, including longevity (Batty, Deary, & Gottfredson, 2007), income (Strenze, 2007), and academic achievement (Deary, Strand, Smith, & Fernandes, 2007).

Within psychometrics, the existence of a general factor of intelligence is undisputed (Jensen, 1998; Spearman, 1927). A person's score on different tests of mental ability will correlate, so that a person who tends to do well on one kind of test will also tend to do well on others. *g* is calculated by applying factor analysis to a variety of cognitive tests, and is fairly stable across different methods of factor analysis (Jensen & Weng, 1994). *g* is also stable across different batteries of test; so that five different test batteries administered to the same group of people yield comparable *g*s, correlating at about $r \sim .95$ (Johnson, Nijenhuis, & Bouchard Jr, 2008). Psychometric *g* is therefore a highly stable construct.

Because *g* is so consistently observed, it has been incorporated into modern intelligence models for which there is empirical support. These include the Verbal-Perceptual-Image Rotation model (VPR model; Johnson & Bouchard, 2005; Vernon, 1965) and the widely-used Cattell-Horn-Carroll model (CHC model, McGrew, 1997). The VPR model is a hierarchical model postulating that *g* explains the greatest amount of variance in secondary verbal, perceptual, and image rotation factors. In the CHC model, *g* explains variance in the second-stratum factors fluid (*Gf*) and crystallized (*Gc*) intelligence. *Gf* is defined as the ability to solve novel problems with general problem-solving abilities, whereas *Gc* is defined as the ability to solve problems by applying previously learned knowledge or techniques. Thus, *g* has backing in different theoretical models.

When a wide variety of cognitive tests are included, *g* typically explains between 30-45% of the total variance (Deary et al., 2010; Helms-Lorenz, Van de Vijver, & Poortinga, 2003). Even very basic cognitive tests of processing speed, such as visual inspection time (assessing whether a stimulus is present or not), are associated with *g* (e.g. Deary, Caryl,

Egan, & Wight, 1989). However, *g* loads particularly highly on to measures of intelligence. *g* typically correlates *r* ~ .75 with the Wechsler Adult Intelligent Scale (WAIS) Vocabulary test, *r* ~ .70 with the Matrix Reasoning test (Hunt, 2010, p. 91), and *r* ~.80 with Raven's Progressive Matrices (Raven & Court, 1998). For this reason, Raven's Progressive Matrices is often used as a proxy for *g* or *Gf* (see Gignac, 2015). Yet employing a proxy test for *g* contradicts the operational definition of *g* as the shared variance between a large number of cognitive tests. Raven's Progressive Matrices require complex cognitive strategies to solve. By contrast, *g* represents the shared variance between a number of tests of varying cognitive complexity. Therefore, in the current paper, 'intelligence' will be used as a general term, and '*g*' or 'psychometric *g*' will only be employed to denote the theoretical construct of general intelligence, or the calculated positive manifold between tests.

Cognitive Models of *g*

The processing speed model of *g*. Despite the strong evidence for a unitary psychometric *g*, the construct is not well understood on the cognitive level. Specifically, it is not clear whether *g* amounts to a single cognitive structure or several. Unitary *g* models have focused on finding a trait which would affect all cognitive abilities (Spearman, 1927). Simple processing speed, as measured by visual reaction or inspection time, presents itself as a likely candidate for such a trait (Jensen, 1998, pp. 203-269; Kail & Salthouse, 1994; Salthouse, 1996). Processing speed is proposed to act as a limiting factor on other cognitive abilities via two mechanisms. Slow processing speed delays the completion of early cognitive processes (the limited time mechanism). This in turn limits the amount of simultaneously available information for higher-level cognitive processing (the simultaneity mechanism; Salthouse, 1996). These mechanisms are proposed to influence working memory, which is hypothesized to have time-dependent components (e.g. Baddeley, Lewis, & Vallar, 1984). Working memory has also been proposed to underlie *g*, due to the high correlation between the two constructs (Colom, Rebollo, Palacios, Juan-Espinosa, & Kyllonen, 2004, though see Ackerman, Beier, & Boyle, 2005). Nevertheless, processing speed mediates the development of working memory (Fry & Hale, 2000; Rose, Feldman, Jankowski, & Van Rossem, 2008), and has been associated with performance on a variety of non-timed tasks, from the domains of memory, reasoning, and spatial ability (Salthouse, 1994). Although processing speed declines with age, and is associated with age-related declines in fluid intelligence, processing speed also appears to mediate cognitive variance within each age group (Salthouse, 1996).

Processing speed mediates the development of cognitive ability in adolescents (Coyle, Pillow, Snyder, & Kochunov, 2011), and mediates within-person cognitive decline in an elderly sample (Sliwinski & Buschke, 1999). Because processing speed mediates the performance on so many timed and non-timed cognitive tests, including tests of working memory; the processing speed model presents itself as parsimonious model for a single ability underlying *g*.

The mutualism model of *g*. The mutualism model presents an alternative account for the existence of psychometric *g*. It is based on the observation that different cognitive processes will inevitably interact dynamically through development, and that this leads to correlated abilities (Van Der Maas et al., 2006). Employing an ecosystem metaphor, the model suggests that strength in a single cognitive process will dynamically affect other abilities. Van Der Maas and colleagues (2006) employed mathematical modelling to compare a model of a single latent factor, to one of dynamically interacting processes, and both were able to explain the positive manifold between cognitive tests. Thus, the model bases itself on the tendency for cognitive processes to correlate through use, and not on the assumption of a unitary underlying cognitive construct.

From studies of cognitive development, there is ample support for the dynamic interaction between cognitive processes. For instance, working memory has been shown to facilitate the use of dual processing strategies for reading comprehension (Just & Carpenter, 1992). In turn, better cognitive strategies promote efficient use of working memory (Siegler, 2005). Studies also show that training children in tasks such as verbalization or the use of the abacus, results in improved performance on Raven's Progressive Matrices (Carlson & Wiedl, 1992; Irwing, Hamza, Khaleefa, & Lynn, 2008).

The processing speed model and the mutualism model give two separate accounts of the positive manifold between abilities. Processing speed affects several other abilities, and should therefore influence *g*. Nevertheless, *g* is estimated to correlate with processing speed at around -.44 to -.52 (Jensen 1998, p. 234). A unitary *g* explanation would presume that a single factor explained up to all variance in *g*. Indeed, even proponents of the processing speed model reject the notion that it is the only cause of variance in *g* (Jensen, 1998, p. 260; Nisbett et al., 2012; Salthouse, 1996). Therefore, it seems unlikely that processing speed is the only underlying factor for *g*. On the other hand, Van Der Maas and colleagues (2006) suggest that processing speed is one of many correlated traits underlying positive manifold.

Nevertheless, understanding the cognitive underpinnings of *g* has its own set of challenges. Tests tend to measure overlapping abilities, and individual cognitive abilities are therefore difficult to isolate (Bartholomew, Deary, & Lawn, 2009; Thomson, 1939). Even between different tests of the same cognitive construct, there are large margins of error (Schmiedek, Lövdén, & Lindenberger, 2014). A better approach to understanding the underpinnings of *g* may therefore be to map the underlying neurobiological structures.

Brain Morphometry associated with *g*

A multitude of neurobiological studies have been conducted on various measures of intelligence, of which a subset specifically examine *g*. The relationship between brain volume and intelligence are among the earliest neuroscientific findings (Galton, 1869). Point estimates of the correlation converge at around $r = .33$ (McDaniel, 2005). Brain volume is a function of the number of cortical neurons as well as the degree of myelination, and together these are thought to mediate information processing capacity (Roth & Dicke, 2005). Therefore both grey and white matter are expected to influence total brain volume and intelligence. Below we review structural neuroimaging studies of intelligence examining grey and white matter. Due to the broadness of the subject matter, we restrict ourselves to covering the most important research findings. Functional studies are not reviewed here.

Grey matter associations with intelligence. Grey matter associations with intelligence have been well-documented, especially in studies which measure voxel-based morphometry (VBM; see Basten, Hilger, & Fiebach, 2015) and cortical thickness (e.g. Choi et al., 2008; Karama et al., 2009; Narr et al., 2007; Tamnes et al., 2011). Volume, as measured by VBM, is a product of both cortical thickness and cortical surface area. Nonetheless, VBM is suggested to be more indicative of cortical surface area than cortical thickness (Sanabria-Diaz et al., 2010). Furthermore, the association between volume expansion and intelligence has been estimated to be largely mediated by cortical surface area expansion (Vuoksimaa et al., 2014). However, cortical surface area and intelligence have been examined in relatively few studies (e.g. Colom et al., 2013; Fjell et al., 2013; Román et al., 2014; Schnack et al., 2015). These studies show that volume and cortical surface area increase in largely overlapping regions, as opposed to cortical thickness which is associated with different regions (Colom et al., 2013; Román et al., 2014).

The Parieto-Frontal Integration Theory (P-FIT) is a widely accepted model mapping the cortical regions associated with intelligence (Jung & Haier, 2007). The model is based on a meta-study of 37 functional and structural neuroimaging studies. The P-FIT suggests that a

network of circumscribed regions within the frontal, parietal, and less frequently temporal and occipital regions are associated with intelligence. Based on these associations, the P-FIT proposes that intelligent behaviour follows a specific cortical path, where sensory information is first processed in occipital (BA 18, 19) and temporal (BA 21, 37) regions, then integrated and abstracted within the parietal cortex (BA 7, 39/40), and sent to the frontal cortex (BA 6, 9, 10, 45-47) for reasoning and problem solving, while the anterior cingulate (BA 32) inhibits and selects the alternative response as required. A recent meta-study has confirmed the importance of these regions (Basten et al., 2015). However, there is considerable variability between studies, and only clusters in BA 10 and BA 39/40 are significantly associated with intelligence in more than 50% of studies (Colom, 2007). The P-FIT is based on several measures of intelligence. However, higher-order factors (i.e. *g*) are associated with smaller areas compared to narrower measures of intelligence (e.g. spatial or verbal intelligence; Román et al., 2014). The authors suggest that areas held in common between different types of tasks must necessarily be smaller than each individual task. Another study shows that different measures of intelligence (i.e. *G*f, *G*c, and spatial intelligence) are associated with partly overlapping cortical regions (Colom et al., 2009). Therefore, *g* may not be associated with the exact same cortical areas noted in the P-FIT.

A particularly useful indication of the neurobiological substrates of *g* is lesion studies. Barbey and colleagues (2012) mapped the lesion associations of *g* in 182 neurological patients. They found that lower *g* was associated with lesions in spatial processing areas (right inferior and right superior parietal cortex), motor processing areas (left somatosensory and left primary motor cortex), language areas (bilateral Broca's area and the left superior temporal gyrus), as well as areas associated with working memory (left dorsolateral prefrontal cortex [DLPFC], left inferior and superior parietal cortices, and the left superior temporal gyrus). In a lesion study from 2010 examining 241 patients, Gläscher and colleagues found that deficits in *g* were associated with lesions in the right occipitoparietal junction, and the right primary motor cortex. Thus, both overlapping and unique areas were observed in comparison to the P-FIT.

White matter associations with *g*. The integrity of white matter fibres is associated with nerve conduction velocity (Smith & Koles, 1970; Waxman, 1980), processing speed, and *g*. Although there is regional variation in white matter microstructure, it is very much a global property of the brain. The general factor of white matter microstructure measured in fractional anisotropy (FA; see Aims of the Present Research) explains approximately 38-40% of

variance among white matter tracts (Penke et al., 2012; Penke et al., 2010). Furthermore, studies show that global FA is associated with *g*, and that this effect is mediated by processing speed (Deary et al., 2006; Penke et al., 2012; Penke et al., 2010). Decline in global FA is also a characteristic feature of ageing (Westlye et al., 2009), which may explain age-related decreases in fluid intelligence (Salthouse, 1996). Thus, global white matter integrity appears to be associated with the processing speed component of *g*.

Beyond global integrity, a handful of studies have investigated microstructural properties of major white matter tracts. The superior longitudinal fasciculus (SLF), inferior fronto-occipital fasciculus/inferior longitudinal fasciculus (IFOF/ILF), uncinate fasciculus, corpus callosum, optic radiation/posterior thalamic radiation, cingulum, corona radiata, internal capsule, and corticospinal tract have all been associated with intelligence; though not all within the same studies (Barbey et al., 2012; Chiang et al., 2008; Clayden et al., 2011; Gläscher et al., 2010; Li et al., 2009; Schmithorst et al., 2005; Yu et al., 2008). Both of the aforementioned lesion studies (Barbey et al., 2012; Gläscher et al., 2010) indicate that long association tracts which connect distal cortical regions, i.e. the SLF, uncinate fasciculus, and superior fronto-occipital fasciculus (SFOF), are associated with *g*. Since the synchronized activity of the cortex depends on white matter conductivity, it has been suggested that the cortical regions in the P-FIT network are functionally dependent on white matter tracts. Especially long association tracts (e.g. the SLF, uncinate fasciculus, SFOF) which connect distal regions of the cortex, have been suggested to facilitate communication between these regions (Gläscher et al., 2010; Jung & Haier, 2007).

However, lesion studies do not provide conclusive evidence that the observed grey and white matter lesions are in fact part of the same underlying system for *g*. No studies have hitherto assessed the brain-wide multimodal components of variance on a voxel level, and associated these with intelligence. Thus, it is not clear whether the subset of cortical regions outlined by the P-FIT are part of the same underlying system as white matter microstructure, or whether they make separate contributions to *g*. Processing speed as measured by EEG, and cortical volume appear to make independent contributions to intelligence (Walhovd et al., 2005). In one structural equation modelling (SEM) study measuring VBM and FA in selected ROIs, a model of eight separate neurobiological properties was better able to model psychometric *g*, than models comprised of one or two multimodal factors (Kievit et al., 2012). A recent SEM study showed that a general factor of FA does not explain significant variance in *g* once total brain volume, cortical thickness, iron deposits, and white matter hyperintensity

load were accounted for (Ritchie et al., 2015). Thus, cortical thickness and brain volume appear to make separate contributions to *g*. Nonetheless, the effect of the general factor of FA appeared to be mediated by the other morphometric indices. Given that this was a study of older adults, and that age is associated with a decline in global white matter microstructure, it is possible that the general factor of FA is more predictive of *g* in lower age strata. Taken together, these studies suggest that there are multiple biological structures underlying *g*.

Aims of the Present Research

Using Linked ICA to study *g*. As of today, several morphometric correlates of *g* have been documented. Neurobiological structures may have multimodal underpinnings (Zatorre et al., 2012), and it has been suggested that association tracts interact with cortical regions to mediate intelligent behaviour (Barbey et al., 2012; Gläscher et al., 2010; Jung & Haier, 2007). Yet there has been little research on the neurobiological structures underlying *g*. Thus, we had two aims with the current study: (a) to assess the number of neurobiological structures associated with *g*, (b) and to uncover their multimodal structure.

We employed Linked ICA in order to address these issues. ICA, like factor analysis, is an unsupervised method of data reduction which divides the input data into uncorrelated components of variance (Comon, 1994). Linked ICA has the added benefit of fusing different modalities (e.g. VBM, FA, etc.) before decomposition into multimodal structures (Groves et al., 2011). Another benefit of Linked ICA is that it automatically parses structured noise into its own components (Groves et al., 2011). Linked ICA also uses different spatial maps across different modalities in order to capture dissimilar noise levels, numbers of voxels, and smoothing requirements. As such, the method may be more sensitive to single-modality components or noise than previous ICA methods, which use the same spatial maps across modalities (Groves et al., 2011). Linked ICA has previously been used to study Alzheimer's disease (Kincses et al., 2013), autism (Itahashi et al., 2015; Mueller et al., 2013), and neurodevelopment (Douaud et al., 2014; Groves et al., 2012). Thus, we expect its utility to extend to other paradigms where one might expect see multimodal, brain-wide differences between individuals.

In the current study we fused different grey and white matter modalities from T1-weighted MRI and diffusion tensor imaging (DTI) in the same participants. This included VBM, cortical thickness, and cortical surface area from FreeSurfer. The DTI measures of FA, mean diffusivity (MD), and mode of anisotropy (MO) were also included. As noted above, cortical surface area has been studied less than VBM or cortical thickness in relation to

intelligence. Nevertheless, VBM appears to be closely associated with the volume expansion observed in intelligence (Sanabria-Diaz et al., 2010; Vuoksimaa et al., 2014). Furthermore, surface area and cortical thickness have distinct genetic influences (Panizzon et al., 2009; Winkler et al., 2010), and are statistically separate (Sanabria-Diaz et al., 2010). While the exact neurobiological substrates are unknown, surface area may reflect the number of cortical columns (Sanabria-Diaz et al., 2010), whereas cortical thickness may reflect the neuronal density and myelination within a column (Panizzon et al., 2009; Parent, 1996). Therefore, all three measures were included.

DTI measures the directional unity of water diffusion in the brain, giving an indication of the integrity of white matter tracts (Beaulieu, 2002). The DTI measures FA, MD, and MO were included. FA is sensitive to the degree of unidirectionality in the diffusion of water molecules in the brain, and higher values of FA indicate a higher degree of myelination, fibre density, and axonal diameter. MD measures the average water movement in three dimensions, and is an unspecific yet sensitive marker of neural degeneration, likely caused by a breakdown of cell membranes (Beaulieu, 2002; Le Bihan, 2003). Although FA and MD are mathematical independent measures, they tend to show opposite directionality; where MD increases FA decreases, and vice versa. This is especially the case in major tracts with minimal crossing fibres (Douaud et al., 2011; Groves et al., 2012). MO expresses the shape of the fibres, where low values indicate planar anisotropy, i.e. a “pancake” shape indicative of crossing fibres; and higher values indicate linear anisotropy, i.e. a “cigar shape”. In smaller fibres there tends to be a positive correlation between MO and FA (Groves et al., 2012). Either MD or MO may be more sensitive to white matter integrity. For instance, in distinguishing mild cognitive impairment from Alzheimer’s disease, MO was found to be more sensitive than MD (Douaud et al., 2011).

Hypotheses. There have been numerous neuroimaging studies documenting the relationship between *g* and (a) global white matter microstructure, which is suggested to underlie processing speed; (b) circumscribed regions within the cortex, which are suggested to underlie specific problem-solving abilities; (c) regional white matter microstructure in major tracts, which is suggested to underlie effective communication between regions. Thus, these morphometric indices are associated with different cognitive processes. Since processing speed only explains about half of the variance in *g*, the mutualism model persuasively argues that *g* may be due to the interaction between correlated, but separate cognitive processes (Van Der Maas et al., 2006). This is further supported by the separate

contribution of processing speed and cortical volume to intelligence (Walhovd et al., 2005), and the better fit afforded by multiple neurobiological factors over a one or two-factor model of *g* (Kievit et al., 2012).

We predicted that several Linked ICA components would be associated with *g*. Specifically, we expected to see a component related to global white matter integrity, characterized by increased FA and decreased MD. We also expected to see a component of regional white matter integrity in major tracts identified by previous studies (i.e. IFOF/ILF, optic radiation/posterior thalamic radiation, corpus callosum, cingulum, corona radiata, internal capsule, and corticospinal tract), but especially those seen in lesion studies (i.e. the SFOF, SLF, and uncinate fasciculus; Barbey et al., 2012; Gläscher et al., 2010). There is evidence for a distributed network of cortical regions associated with intelligence. Based on lesion studies, we expected to see a component associated with greater VBM, surface area, or cortical thickness in Broca's areas, the superior temporal gyrus, the DLPFC, the inferior and superior parietal cortices, and the somatosensory and primary motor cortices. Nevertheless, we remain agnostic as to whether these components are multimodal in nature, and whether other modalities will also be present in the expected components.

Materials and Methods

Participants

The study utilized neurocognitive test scores and MRI data from 226 healthy participants, who were recruited for the Thematically Organized Psychosis (TOP) study. Data collection has been approved by the Regional Ethics Committee and the Norwegian Data Inspectorate. Participants were recruited from national registries (www.SSB.no), and all participants gave their informed, written consent.

The age range spanned from 17 to 46 years (mean = 32.14, SD = 7.68), with 41% females. Exclusion criteria were a history of self-reported somatic, mental, or neurological disorders. Participants were also excluded if they expressed concern about their cognitive status, or had a full-scale IQ (FSIQ) below 70. FSIQ calculated from the four Wechsler Abbreviated Scale of Intelligence (WASI; Wechsler, 2007) test scores, was 112.77 (SD = 10.60), with a range of 79 to 135.

Imaging

MRI Acquisition and Preprocessing. Imaging was performed on a 3T GE Signa HDxT scanner with an 8-channel head coil at Oslo University Hospital. T1-weighted data was collected with a 3D Fast Spoiled Gradient Echo (FSPGR) sequence using the following parameters: TR/TE/TI = 7.8 ms/2.956 /450 ms, flip angle=12°. Field of view was 256×256 mm², slice thickness = 1.2 mm, acquisition matrix = 256×192, and reconstruction matrix = 256×256. DTI data was collected with a 2D Spin Echo sequence using the following parameters: TR/TE=15000ms/84.1 ms, flip angle=90°; number of diffusion directions=30; field of view was 240×240 mm², slice thickness=2.5 mm, acquisition matrix=128×128; in-plane resolution = 1.875*1.875.

Preparing Data for Linked ICA. Data segmentations from T1-weighted data were inspected and corrected when required according to standard FreeSurfer procedures (http://surfer.nmr.mgh.harvard.edu; Fischl et al., 2002). Linked ICA was performed in MATLAB using tools provided by the FMRIB centre (http://fsl.fmrib.ox.ac.uk/fsl/fslwiki/FLICA).

Preprocessing T1-w MRI Data. The pipelines recommended by FSL FLICA were utilized for decomposing the data. This was performed on arealization and cortical thickness, VBM (Douaud et al., 2007), and DTI measures FA, MD, MO (Ennis & Kindlmann, 2006). Spatial maps for arealization and cortical thickness were obtained in FreeSurfer, by first

performing brain extraction, intensity normalization, automated tissue segmentation, surface-based cortical thickness estimations, generation of white and pial surfaces, surface topology correction, automated whole-brain segmentation, and spherical interindividual surface alignment (Dale, Fischl, & Sereno, 1999; Fischl & Dale, 2000). Arealization maps were estimated using an automated surface reconstruction scheme (Hogstrom, Westlye, Walhovd, & Fjell, 2012); and cortical thickness was obtained by representing the boundary between grey and white matter and calculating the distance to the cortical mantle (Dale et al., 1999; Dale & Sereno, 1993). VBM maps were generated using FSL-VBM (Douaud et al., 2007). In order to correct for local expansion or contraction, the VBM maps were divided by the Jacobian of the warp field.

Preprocessing DTI Data. DTI data was pre-processed in FSL (Smith et al., 2004; Woolrich et al., 2009) by performing motion-correction; eddy-current distortions; removal of non-brain tissue; and computing FA, eigenvector, and eigenvalue maps. FA was skeletonized to the mean FA volume, and all volumes (FA, MD, MO) were warped to a common template (FMRIB58_FA) using Tract-Based Spatial Statistics (TBSS; Smith et al., 2006).

Downsampling. All spatial maps across modalities were downsampled for ease of computation before performing Linked ICA. The spatial maps for arealization and cortical thickness were resampled to a common coordinate system (fsaverage5), and smoothed with a Gaussian kernel with a full width of half maximum of 15 mm for cortical thickness and 10 mm for surface area. The VBM spatial maps were resampled from 2 mm to 4 mm, and then smoothed with an isotropic Gaussian kernel with a full width of half maximum of 9.76 mm. TBSS skeletons were downsampled from 1 mm to 2 mm.

Linked ICA

Linked ICA was performed in MATLAB (v. R2013b). Previous studies have found that between 50 and 100 components are able to robustly model variance (Groves et al., 2012). Including too few components fails to capture meaningful variance, and including too many will split up meaningful components. Therefore, both 50 and 100 components were derived in two separate runs. These were then compared through visual inspection. Bayesian PCA (Bishop, 1999; Choudrey & Roberts, 2001) employs spherical noise modelling, which reduces each modality to an optimal number of spatial maps, and separate noise components. The components were iteratively computed based on the tensor products of the spatial map × modality weight × subject weight, and orthogonally rotated in order to explain all the spatial

data. For each subject for each component, a subject-course was estimated, reflecting the individual participants' contribution or weight to each of the components. These subject weights were submitted to cross-subject statistics to assess associations with the cognitive data. The subject-courses were fit back into the original datasets to derive the final set of spatial maps, and subject-courses were converted to pseudo-Z-statistic. Each modality in each component had a weighting, given in percent, indicating the weighting of the modality in the component.

Post-processing. Component maps were thresholded a $3 < |z| < 10$ for visualization, and clusters were anatomically characterized using the Harvard-Oxford Cortical Structural Atlas (http://www.fmrib.ox.ac.uk/fsl) and the ICBM-DTI-81 White-Matter Label Atlas (Mori et al., 2008), provided with FSL. All components' spatial maps were manually inspected. In any given component, if all modalities were deemed noisy, they were eliminated. The criteria for being deemed a noise or an artefact component were scattered activation throughout the spatial map with no major clusters, and isolated activity around the skull or blood vessels at the thalamus or brainstem.

Estimation of *g*

Psychometric *g* was derived by applying factor analysis to a variety of tests from the Norwegian version of the WASI, D-KEFS Color Word Interference task (Delis, Kaplan, & Kramer, 2001), and the Matrics Consensus Cognitive Battery (MCCB; Kern et al., 2008; Nuechterlein et al., 2008). These sampled specific cognitive domains, i.e. verbal and perceptual intelligence, working memory, attention, and cognitive processing speed (i.e. timed performance on cognitive tasks). Raw scores from 16 tests were used in the factor analysis (see Table 1). Tests were excluded if they showed strong ceiling effects (mode = max value), in order to accurately model upper-range intelligence. *g* is often calculated from several Wechsler Intelligence subtests (Hunt, 2010, p. 91-97). In our study 16 tests were used, including several Wechsler Intelligence subtests, or nearly identical tests (e.g., BACS Symbol coding/WAIS-III Digit-symbol coding and LNS/WAIS-III LNS). Detailed descriptions of the tests are given in Appendix A.

Table 1
Neurocognitive tests included in the study

Broad domain	*Neurocognitive test*	*Cognitive domain*
Intelligence	WASI Vocabulary	verbal intelligence
	WASI Similarities	verbal intelligence
	WASI Block Design	perceptual intelligence
	WASI Matrix Reasoning	perceptual intelligence
	NART	verbal intelligence
Working and short-term memory	WAIS-III Digit Span backwards condition	auditory working memory
	WMS-III Spatial memory sequencing forwards condition	spatial working memory
	BVMT-R Immediate condition	visuospatial working memory
	Letter-Number Span	auditory working memory
Attention	CPT-IP 4-digits d'	attention, working memory
	D-KEFS CWIT Inhibition condition	inhibitory control
Learning/ memory	HVLT-R Immediate condition	verbal short-term memory
	WMS Logical Memory I Story	auditory short-term memory
Processing speed	Trail Making Test Part A	visual scanning, visuomotor tracking, cognitive shifting
	BACS Symbol Coding	working memory
	Word Fluency: Animal Naming	verbal fluency

The current study employed Principal Axis Factoring (PAF), which explains the common variance between items, and is frequently employed as a method for calculating *g* (e.g. Barbey et al., 2012; Colom, Abad, Garcıa, & Juan-Espinosa, 2002; Deary et al., 2007). Furthermore, PAF does not require normally distributed data (Fabrigar, Wegener, MacCallum, & Strahan, 1999). Nonetheless, *g* is fairly stable across different methods of factor analysis (Jensen & Weng, 1994). PAF was performed with the 16 variables with no rotation, and the first factor was interpreted as *g*. Statistical analysis was carried out using IBM SPSS v. 22.

Statistical Analysis

The demographic characteristics of *g* were assessed by performing a three-step hierarchical multiple regression with covariates age (linear and quadratic), gender, and *years of education*, introduced in this order. Because brain structure ages in a nonlinear trajectory (Westlye et al., 2009), both linear and quadratic age terms were included in the models. The use of a hierarchical multiple regression allowed us to assess the specific associations at each step between control variables and *g*, and also control for these associations when determining the correlation between *g* and years of education.

In order to assess which components were associated with *g*, individual one-step GLMs were performed for *g*, entering age (linear age and age squared), gender, and each separate component per GLM. After subtracting artefact components, 34 GLMs were performed in total. Linked ICA components which were associated with *g* at a significance level of $p < .05$ were considered nominally associated. The association between *g* and the components were corrected for multiple comparisons with the False Discovery Rate (FDR) procedure (Benjamini & Hochberg, 1995) in MATLAB.

To assess whether any component was differentially associated with *g* between genders, the file was split by gender. Then, the correlation coefficient between *g* and each component was compared using a Fisher's *r*-to-*z* transformation.

To assess the total amount of variance in *g* explained by all the components, a three-step hierarchical multiple regression was performed for *g* with age, gender, and all components combined. A second three-step hierarchical multiple regression was performed after the same procedure, but only including the components which were nominally significantly associated with *g* ($p < .05$).

Finally, three-step hierarchical multiple regressions were performed for each nominally significant component, assessing associations with age, gender, and FSIQ. This was done in order to understand the demographic characteristics of the components. FSIQ was included in order to assess whether any components were uniquely associated with *g*.

Results

Demographic Features

The average of the four unstandardized WASI intelligence scores was used to calculate FSIQ. There was a positive, linear relationship between age and FSIQ (β =.184, $t(224)$ = 2.805, p = .005), indicating that in our sample, older people had higher FSIQ. There was no significant association between gender and FSIQ when controlling for age (β = -.087, $t(222)$ = -1.356, p = .176).

Linked ICA

Two runs with different dimensionalities, L = 50 and L = 100 were performed. It was not a priori clear which run would be more appropriate to the sample. However, the more heterogeneous the sample, the more dimensions would likely be required to capture the variance in the imaging data. The spatial maps derived from the two runs were compared through visual inspection. L = 100 split the components derived from L = 50, and created more noise components. This indicated that 100 components were excessive for the purpose of describing the data, so the L = 50 run was utilised instead. Components were ordered after the amount of explained energy. The components are shown in Figure 1, which should be interpreted as a scree plot.

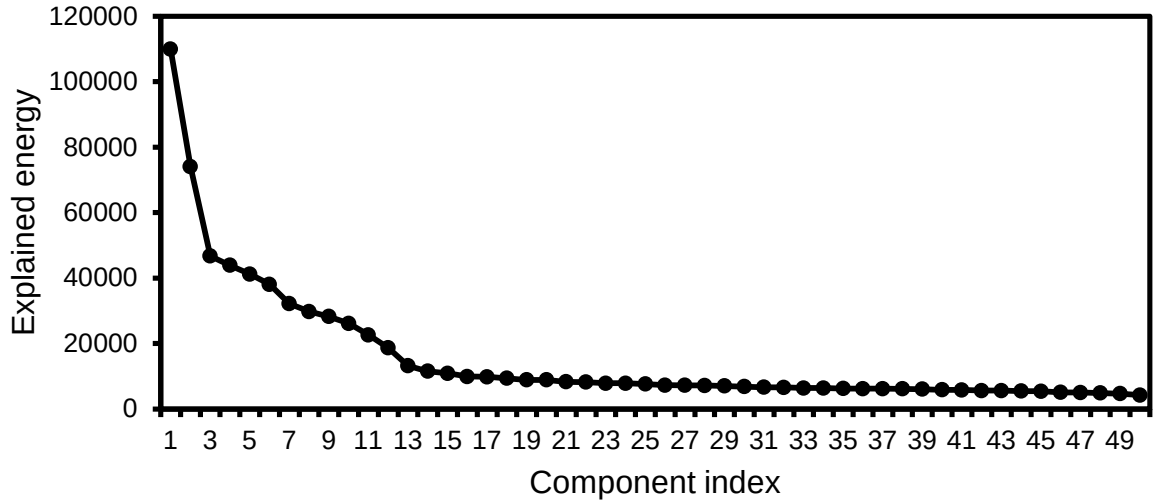

Figure 1: Total energy explained by each component. The figure shows the components ordered after the amount of spatial variance, or energy, which they explained. The first components reflected global morphometric differences. Distinct breaks can be observed after component 3 and 13. Note that Figure 1 also depicts noise components.

Components 2, 3, 4, 6, 9, 10, 11, 34, and 47 were associated with high single-subject loadings (10-90% of the total variance was explained by one subject). In other words, these components were most likely explaining structural abnormalities associated with a single participant. These participants were visually inspected in FSL, and large ventricles, artefacts due to metal, and other structural abnormalities were observed. Therefore, the aforementioned components were excluded.

Component 18, 28, 33, 39, 40, 46, and 50 were structured noise components, characterized by noise in the skull beneath the ventromedial frontal regions, and around the brain stem and thalamus. This likely reflected EPI-related geometrical distortions, as well as vessels. This was apparent only in the DTI-modalities, and since there were no meaningful cortical modalities in the component, the components were interpreted as noise and discarded. This left 34 non-artefact components. Figure 2 shows an example of a non-artefact component (C1) as well as an artefact component (C40).

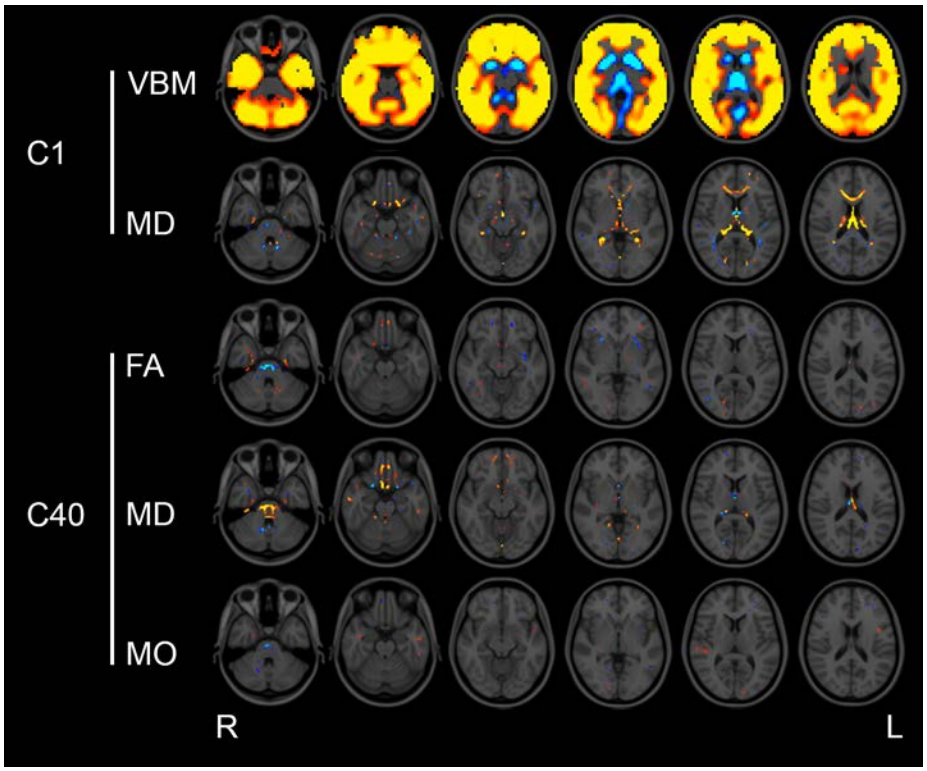

Figure 2: Visual description of neuroanatomy for C1 and C40. Axial view of C1 (non-artefact component) and C40 (artefact component). C1 explained the greatest amount of energy of all components, and was characterized by global grey matter density (VBM) across the brain and MD in the corpus callosum, thalamus, and ventricles. C40 was characterized by DTI-driven noise around the skull and the vessels in the brain stem. The other modalities did not explain much variance in the component (< 2%). Subsequently the component was discarded.

Principal Axis Factoring.

PAF was performed with the 16 tests, with no rotation. Kaiser-Meyer-Olkin Measure of Sampling Adequacy yielded a score of .864; which implies that the rotation and number of factors was accurate (Hutcheson & Sofroniou, 1999). Bartlett's Test of Sphericity was χ^2 (120) = 1035.184, $p < .0001$. The highly significant *p*-value indicated that the items were sufficiently correlated to be included in the factor analysis. The unrotated factor matrix, displaying the correlations between the tests and the first factor, is presented in Table 2. Only the first factor, representing *g*, was analysed further. The first factor explained 31.31% of the total variance, consistent with typical estimates of *g* (Helms-Lorenz et al., 2003). FSIQ was significantly correlated with *g* ($r = .819$, $p < .0001$). Thus, the computed *g* was considered a valid representation of general intelligence.

Table 2
PAF Unrotated Factor Matrix

Factor loadings between tests and Factor 1	*Factor 1*
WASI Vocabulary	.626
WASI Similarities	.601
WASI Block Design	.616
WASI Matrices	.563
NART	.578
WAIS-III Digit Span backwards	.504
MCCB Letter-Number Span	.405
MCCB WMS Logical Memory I Story	.491
MCCB WMS-III Spatial memory sequencing forwards	.646
MCCB BVMT-R Immediate condition	.449
MCCB HVLT-R Immediate condition	.553
MCCB CPT-IP 4-digits d'	.504
MCCB D-KEFS CWIT Inhibition	.434
MCCB Trail Making Test Part A	.438
MCCB BACS Symbol Coding	.567
MCCB Word Fluency: Animal Naming	.391

Regression Analyses

A three-step hierarchical multiple regression was performed for *g*; with age (linear and quadratic), gender, and years of education, entered, in this order. Age explained a significant proportion of the variance in *g*, (R^2= .038, *F*-change (2, 223) = 4.369, *p* = .014). *g* increased linearly with age (β = 1.609, *t*(223) = 2.719, *p* = .007), though a negative quadratic relationship was also observed (β = -1.553, *t*(223) = -2.573, *p* = .011). Thus, *g* follows an inverse U-curve with age. Entering gender as a second variable did not explain significantly more variance as measured in R^2-*change* (R^2 = .038, R^2-*change* =.000, *F*-change (1, 222) = .007, *p* = .934). However, *years of education* did explain significantly more variance in *g* (R^2 = .148, R^2-*change* =.110, *F*-change (1, 221) = 28.479, *p* < .001). The final model, including age, gender, and *years of education*, is given in Table 3.

Table 3
Regression of g with demographic variables

	Model 3				
Variable	*B*	*SE(B)*	*β*	*t*	*p*
(Intercept)	-3.253	1.147		-2.835	.005
Age	.059	.078	.456	.761	.447
Age squared	-.001	.001	-.503	-.851	.395
Gender	.005	.126	.002	.038	.970
Education	.168	.031	.377	5.337	.000

Note. B = unstandardized beta, SE = standard error of B, $\overline{\beta}$ = standardized beta. For "Gender"; males = 1, females = 2. "Education" = years of education.

Analyses of all Components

To test which components were significantly associated with *g*, a GLM was performed with each of the 34 non-artefact components, while controlling for age (linear and quadratic) and gender. The following three components were significantly ($p < .05$) associated with *g*: Component 8 (C8; $R^2 = .019$, $F(1, 221) = 4.189$, $p = .042$), Component 20 (C20; $R^2 = .032$, $F(1, 221) = 7.225$, $p = .008$), and Component 48 (C48; $R^2 = .026$, $F(1, 221) = 6.015$, $p = .015$. Scatter plots between *g* and the individual subject weights on these components are given in Figure 3. Figure 4-6 shows the spatial maps of C8, C20, and C48. A full description of the ten greatest clusters for each modality, including coordinates and anatomical labels, are given in Appendix B. The DTI modalities tended to load more heavily on to the components, possibly reflecting the higher degree of variance in the DTI data input.

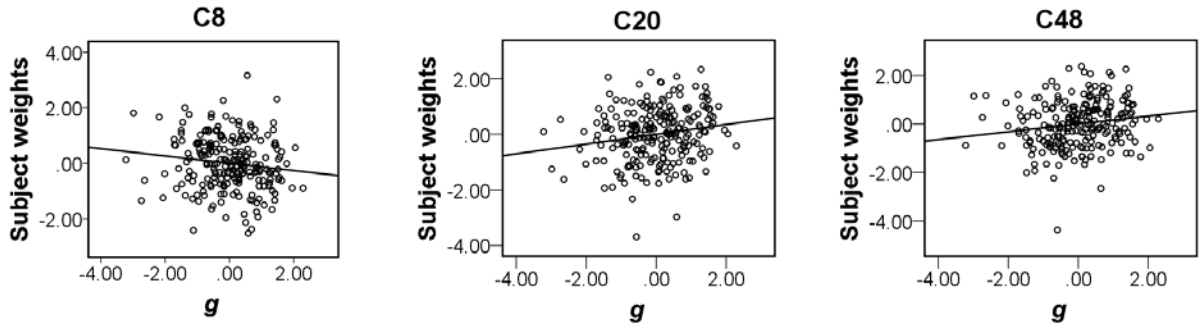

Figure 3: Scatter plots showing the relationship between *g* and independent component subject weights for C8, C20, and C48; after correcting for age and gender**.** Scatter plots for C8, C20, and C48. A negative relationship was observed for C8 ($R^2 = .018$), while a positive relationship was observed for C20 ($R^2 = .030$) and C48 ($R^2 = .023$).

When the *p*-values from the 34 GLMs were corrected for multiple comparisons, no effects survived FDR correction. Nevertheless, components showing nominally significant associations ($p < .05$) were retained for further analysis.

To assess whether gender mediated the association between *g* and any of the components, the 34 GLMs were rerun as above while also introducing the interaction term gender*component into the model. C8, C20, and C48 did not show a significant interaction effect ($p < .05$). However, C8 showed a trend towards significance, where C8 was more predictive of *g* for females (β = -.252, $t(220)$ = -1.879, p = .062). Gender differences were not analysed further in this study.

To assess the total amount of variance that the components explained in *g*, a two-step hierarchical regression was run for *g* with age and gender first; then with the 34 components. The demographic variables alone were significantly associated with *g*, (R^2= .042, $F(3, 222)$ = 2.902, p = .023). Entering the 34 components increased the explained variance from 4.2% to 22.6%, though this did not significantly improve the model (R^2 = .226, R^2 -change = .184, *F*-change (34, 191) = 1.359, p = .106). A second two-step regression was run for *g* with the demographic variables first, and then components C8, C20, and C48. This time, the three components significantly improved the model (R^2= .102, R^2 -change = .060, *F*-change (6, 219) = 4.838, p = .003), and explained variance increased from 4.2% to 10.2%. Thus, a number of components beneath the threshold of significance explained a large proportion of variance in *g*.

Analyses of Significant Components

Descriptive analyses were performed in order to understand how different variables such as age and gender were associated with C8, C20, and C48. We also assessed how the different variables were associated with FSIQ. Psychometric *g* was, as expected, highly correlated with FSIQ; yet it was not certain that subject weights on each component would be associated with FSIQ. In order to explore the possibility that certain components were uniquely associated with *g*, FSIQ was included as the final step in a hierarchical regression analysis, following age and gender. A description of each component is given below, together with the hierarchical regression analyses.

Component 8. C8 represented global decreases in white matter integrity, reflecting higher MD (82%) with lower FA (17%). Both MD and FA represented one major cluster spanning the whole brain, though FA had less voxels than MD. MD represented all major

tracts in the ICBM-DTI-81 White-Matter Label Atlas. FA was represented in most tracts, though some minor tracts were not represented.

A three-step hierarchical regression was performed with age (linear and quadratic), gender, and finally FSIQ. Age was able to predict a significant proportion of variance in C8 (R^2 =.035, F (2,223) = 4.023, p=.019). A negative linear association was observed between C8 and linear age (β = -1.104, t(223) = -1.862, p = .064), a as well as a positive quadratic relationship (β = .956, t(223) = 1.613, p = .108). Gender did not explain significantly more variance in C8 (R^2 = .035, R^2-*change* =.000, F-change (1, 222) = .004, p = .953). However, entering FSIQ did (R^2 = .071, R^2-*change* =.036, F-change (1, 221) = 8.549, p = .004). Table 4 presents the third model. As with *g*, FSIQ was negatively associated with C8.

Table 4
Regression of C8 with demographic variables

	Model 3				
Variable	*B*	*SE*	*β*	*t*	*p*
(Intercept)	1.587	1.193		1.330	.185
Age (linear)	-.083	.076	-.661	-1.095	.275
Age (squared)	.001	.001	.546	.908	.365
Gender	-.041	.128	-.021	-.325	.745
FSIQ	-.256	.087	-.199	-2.924	.004

Table 4: B = unstandardized beta, SE = standard error of B, β = standardized beta. For "Gender"; males = 1, females = 2. FSIQ significantly decreased as subject weights on C8 increased.

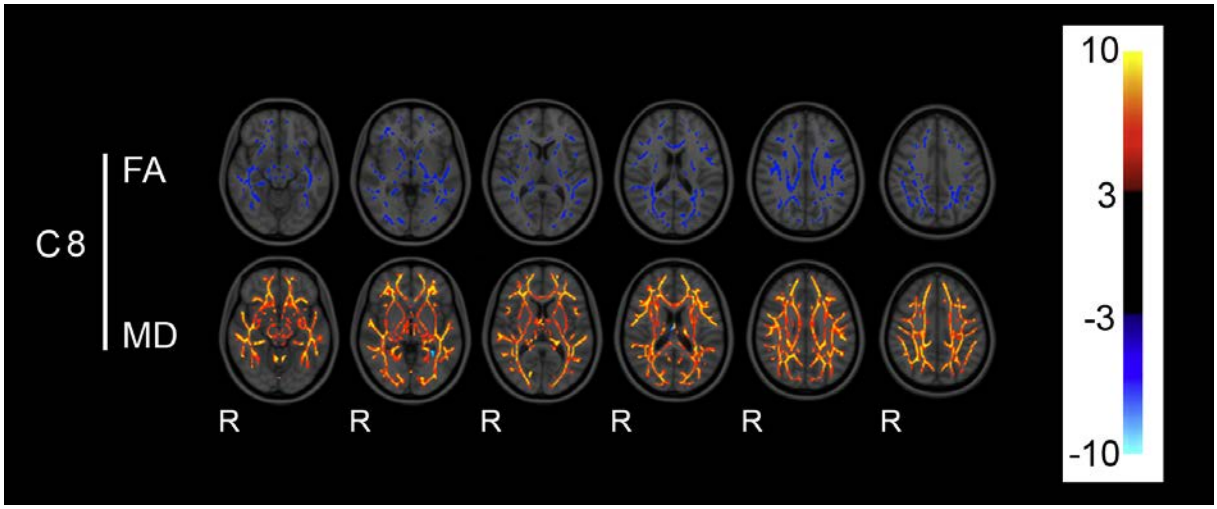

Figure 4: Visual description of neuroanatomy of C8. C8 was characterized by global white-matter integrity as indexed by FA and MD with opposite weightings. Axial view.

Component 20. C20 was characterized by higher FA (32%) and MO (31%) in mainly association, projection, and commissural pathways. Higher FA was observed in the IFOF/ILF, corpus callosum, cingulum, fornix, anterior corona radiata, internal capsule, SLF, uncinate fasciculus, and corticospinal tract. The greatest cluster encompassed the right anterior corona radiata, right cingulum, left fornix, left internal capsule, and left IFOF/ILF. The greatest decrease in MD (17%) was observed in the bilateral corpus callosum. A concurrent decrease in volume (9%) was observed in all of the frontal and temporal cortices; as well as specific parietal, insular, cingulate, and occipital areas. Cortical thickness (6%) decreased in regions within the frontal, parietal, insular, cingulate, and temporal areas. FA also increased in the left precuneus, left postcentral gyrus, and right supramarginal gyrus.

A three-step hierarchical multiple regression was performed for C20 with age (linear and quadratic), gender, and FSIQ. The component was not significantly associated with age (R^2 = .021, F(2, 223) = 2.441, p = .089). However, gender explained significant variance in the component (R^2 = .046, R^2-*change* =.025, F-change (1, 222) = 5.760, p = .017). Males had significantly higher subject weights on C20 than did females. FSIQ also explained significant variance in the component (R^2 = .073, R^2-*change* =.027, F-change (1, 221) = 6.438, p = .012). Table 5 presents the third model with all demographic variables.

It was suspected that the decrease in grey matter volume and thickness might be due to an interaction between normal neurobiological development and cognitive development. Therefore a post-hoc GLM was performed for C20 with *g*, gender, age (linear and quadratic), and the interaction term *g* by age. The interaction term did not predict significant variance in C20 (R^2 = .006, F(1,220) = 1.397, p = .238).

Table 5
Regression of C20 with demographic variables

	Model 3				
Variable	*B*	*SE*	*β*	*t*	*p*
(Intercept)	-1.199	1.223		-.980	.328
Age (linear)	.105	.078	.815	1.352	.178
Age (squared)	-.002	.001	-.794	-1.323	.187
Gender	-.286	.131	-.143	-2.189	-.030
FSIQ	.227	.090	.173	2.537	.012

Table 5: B = unstandardized beta, SE = standard error of B, β = standardized beta. For "Gender"; males = 1, females = 2. FSIQ was positively associated with C20 subject weights. Males had higher C20 subject weights than females.

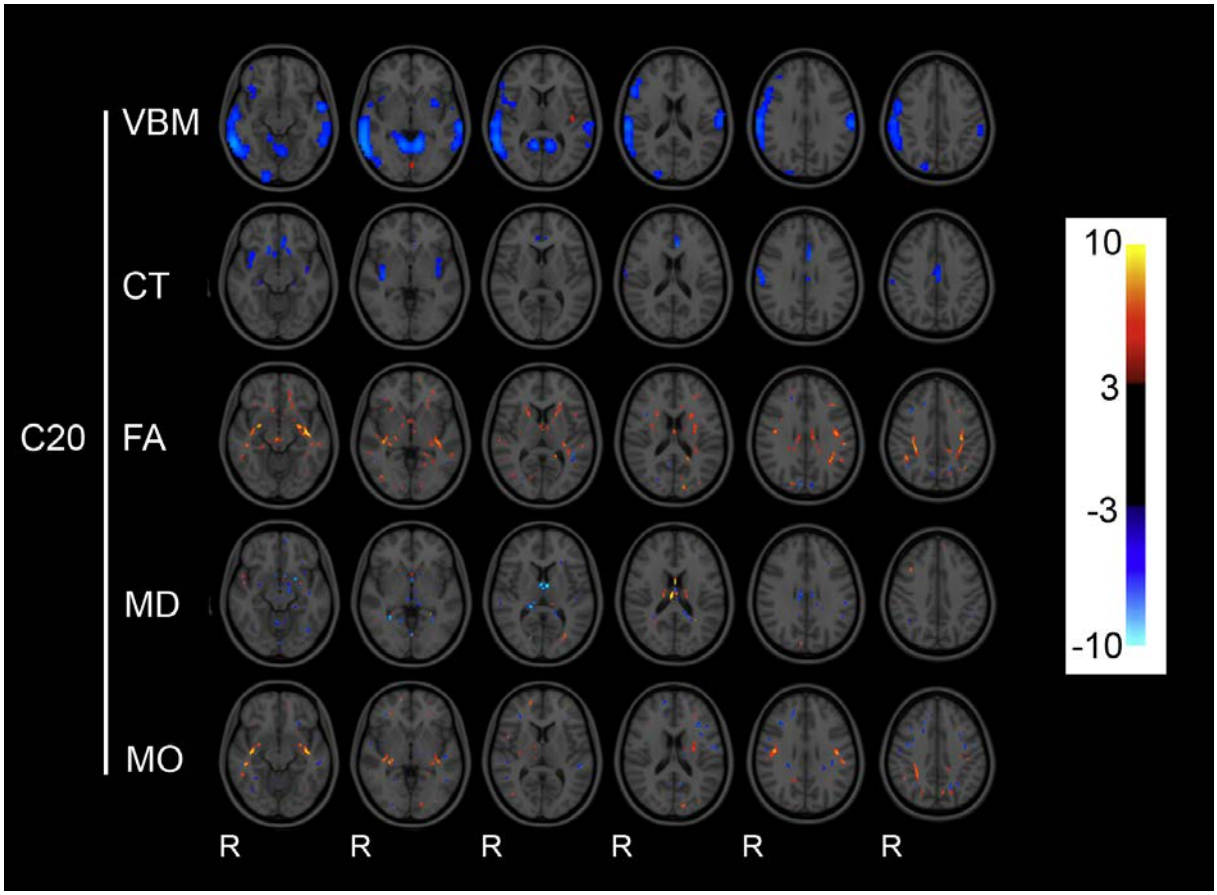

Figure 5: Visual description of neuroanatomy of C20. C20 was characterized by higher FA in major tracts and a concurrent decrease in VBM and CT. "CT" = cortical thickness. Axial view.

Component 48. C48 was represented by increases in surface area (7%) across a distributed network of cortical regions in the frontal, temporal, parietal, and occipital cortices (see Figures 6 and 7). Surface area expansion was observed within the bilateral frontal cortices (BA 9, 44, 45, 47), middle temporal regions (BA 20), bilateral inferior parietal regions (BA 22, 40), and the right lateral occipital cortex (BA 37). Surface area diminished in the bilateral middle frontal gyri (BA 46). Volume decreased (6%) in predominantly the left hemisphere counterparts to regions of surface area expansions (i.e. the supramarginal gyrus, frontal pole, and inferior and middle frontal gyrus), though it also increased in the precuneus, left occipital pole; and right temporal fusiform cortex. White matter diffusion changes in FA (30%) and MD (22%) were observed in commissural and projection pathways. The bilateral corpus callosum, right lingual gyrus and right corticospinal tract were associated with higher white matter integrity, whereas the left-hemisphere counterparts were associated with lower

integrity. Higher FA was also observed in the left parahippocampal gyrus, left precuneus, bilateral inferior temporal gyri, and left superior frontal gyrus.

A three-step hierarchical regression was performed for C48 with age, gender, and FSIQ. None of the variables explained significant variance in C48. The third model with all variables included was also insignificant R^2 = .035, $F(4, 221) = 2.011$, p = .094. Thus, despite the strong association between *g* and FSIQ in the current study, C48 was not associated with FSIQ. Consequently, we performed a post-hoc analysis to assess whether C48 was differentially associated with high and low FSIQ. The file was split above and below median FSIQ. Two GLMs were performed for C48 with age, gender; and high and low FSIQ separately. C48 was positively associated with high FSIQ (β = .133, $t(221) = 1.385$, p = .169), and negatively associated with low FSIQ (β = -.140, $t(221) = -1.502$, p = .136), though none of the associations reached significance. The two standardized betas for high and low FSIQ were compared using Fisher's *r*-to-*z* transformation. The difference was statistically significant (z = 2.037, two-tailed p = .042).

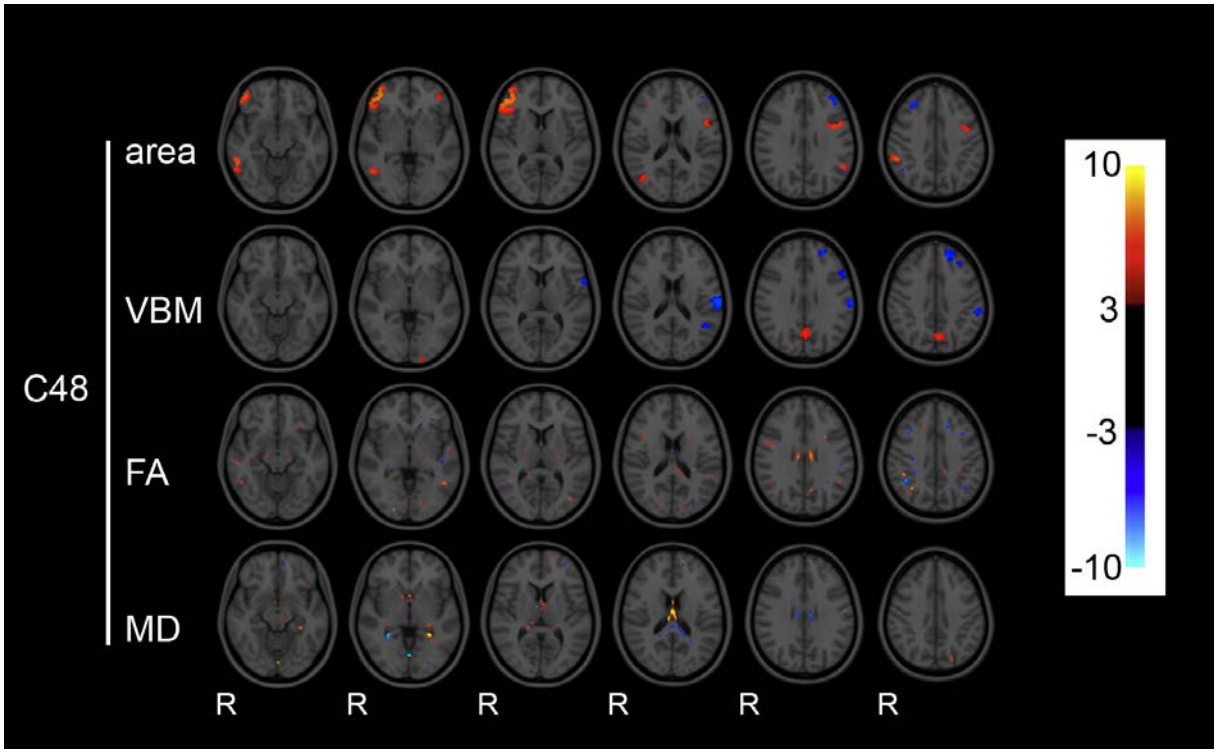

Figure 6: Visual description of neuroanatomy of C48. C48 was characterized by surface expansion and FA and MD changes in commissural tracts. The MO modality was omitted, as there were no visible clusters. "CT" = cortical thickness. Axial view.

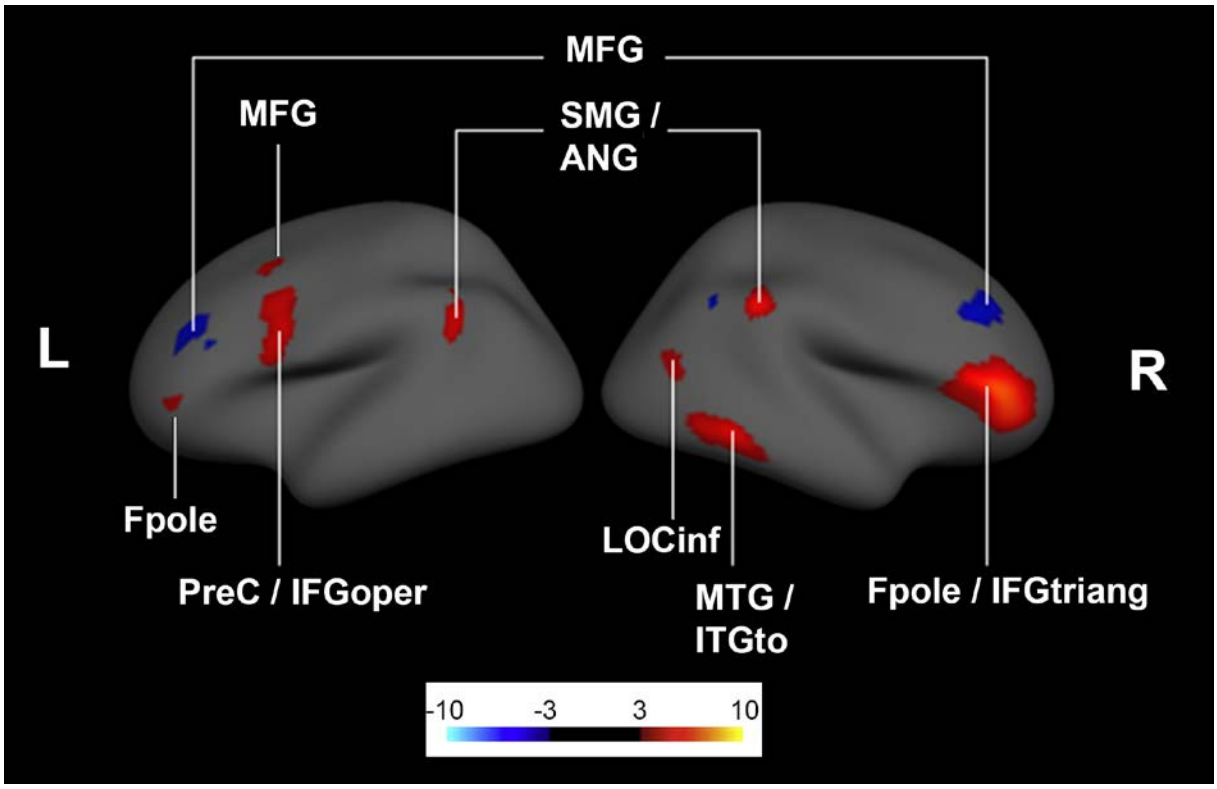

Figure 7: Lateral view of the surface arealization modality of C48. C48 shows localized modes of variability in arealization in the following regions: the bilateral frontal poles and the right inferior frontal gyrus, pars triangularis (Fpole/IFGtriang); the left precentral gyrus/inferior frontal gyrus, pars opercularis (PreC/IFGoper); the right midldle and inferior temporal gyrus, temporooccipital part (MTG/ITGto); the bilateral supramarginal gyri and right angular gyrus (SMG/ANG); the bilateral middle frontal gyri (MFG); and the lateral occipital cortex, inferior division (LOCinf).

Discussion

The goal of the current study was to assess the multimodal structural brain patterns underlying *g*. Although no components survived corrections for multiple comparisons, three components were nominally associated with *g*: a global white-matter integrity component (C8), a component of increased integrity in specific white matter tracts (C20), and a component of increased surface area in a distributed network of cortical regions (C48). These conformed largely to the hypothesized components. The structural makeup of each significant component is discussed in further detail below.

The three significant components alone explained 6% of the variance in *g*. However, when all 34 variables were included, this explained a total of 18.4% of the variance in *g*. It is very interesting that not one single brain component is able to explain *g*, but that a combination of all non-artefact components explains a large proportion. Thus, a considerable amount of variability in *g* can be attributed to variability in brain structure, even in a homogeneous and relatively young and healthy sample. This neurobiological variability is not captured by a single component, but rather by a combination of several components. The implications of these findings will also be discussed.

Global White Matter Component (C8)

We predicted a component related to global white matter integrity, which was observed in C8. Besides being associated with *g*, C8 was associated with age in a U-shape trajectory, whereby white matter integrity increased with age up to a certain point before decreasing. This accords well with previous observations of the inverted-U age trajectory of global FA (Westlye et al., 2009), and of age-related declines in processing speed and fluid intelligence (Salthouse, 2000). An inverted-U age trajectory was also observed for *g* in the current study. Thus, C48 appears to relate to normal processing speed decline with to age, but also to individual differences in processing speed related to cognition. C48 may also be compared to the first component from Groves and colleagues (2012) Linked ICA study, showing global white matter integrity with a U-shaped age association. The authors note that although their component was significantly associated with age, it had a “noisier” age trajectory than some of the other components. They attribute this to other extraneous factors which might influence the component, of which processing speed differences within each age group is a likely candidate. C8 is also comparable to the brain-wide FA factor found through principal component analysis (PCA) by Penke et al. (2012), which was associated with *g* and mediated

by processing speed. However, the current study was not able to assess the component's relationship with measures of processing speed. Measures of *cognitive processing speed* were included in the PAF (see Appendix A), but these tests also reflect other cognitive processes besides simple processing speed. Therefore, the suggested link between C8 and processing speed must remain hypothetical.

Regional White Matter Component (C20)

C20 reflected higher FA and MO in major projection, association, and commissural tracts in the brain, connecting different regions of the cortex. We observed the predicted white matter tracts (IFOF/ILF, corpus callosum, cingulum, fornix, anterior corona radiata, internal capsule, SLF, uncinate fasciculus, and corticospinal tract) in one or more of the FA clusters. Contrary to expectations, we did not observe the SFOF or the posterior thalamic radiation.

The corticospinal tract is part of the internal capsule and corona radiata, and carries signals from the motor cortex to the spinal chord. The internal capsule and corona radiata are comprised of both ascending and descending neurons, and connect to the cortex in a fan-like shape (Catani, Howard, Pajevic, & Jones, 2002). The IFOF/ILF connects the frontal regions to the posterior temporal and occipital regions, and is part of the visuospatial attention network (Urbanski et al., 2008; Wakana, Jiang, Nagae-Poetscher, Van Zijl, & Mori, 2004). The cingulum connects the frontal regions to the precuneus, hippocampus, and parahippocampus (Wakana et al., 2004), and is important for motivation (Bush, 2011). In conjunction with the fornix and other medial regions, the cingulum is also important for spatial and episodic memory (Albo, Di Prisco, & Vertes, 2011; Markowitsch, 2005). The SLF and uncinate fasciculus are long association bundles. The SLF connects the frontal, temporal, parietal, and occipital lobes. The uncinate fasciculus connects the temporal cortex to the limbic regions (hippocampus and amygdala), and to the orbitofrontal cortex (Wakana et al., 2004). The corpus callosum integrates information between the two hemispheres (Bloom & Hynd, 2005). White matter integrity in all these tracts have previously been associated with intelligence (Barbey et al., 2012; Chiang et al., 2008; Clayden et al., 2011; Gläscher et al., 2010; Li et al., 2009; Schmithorst et al., 2005; Yu et al., 2008).

Possible interaction between age and *g*. The component also showed grey matter volume reduction and cortical thinning in broad swathes of frontal, temporal, parietal, and occipital areas. It was suspected that this might be due to the interaction between cognitive development and normal cortical development. White matter tissue volume increases linearly

into early adulthood (Lebel & Beaulieu, 2011), whilst cortical thickness and volume decreases across the brain, especially in frontal and parietal cortices (Østby et al., 2009). Two mechanisms have been proposed to explain these findings. Firstly, pruning is a developmental process which is suggested to reduce underused synapses in the cortex whilst axonal myelination increases (Huttenlocher, 1990; Huttenlocher & Dabholkar, 1997). Secondly, proliferation of myelin into the cortical neuropil has been hypothesized to push the border between grey and white matter outward (Sowell et al., 2004). This will purportedly give the appearance of grey matter reduction, without actually entailing a reduction in size or number of grey matter neurons.

Normal trajectories of cortical development interact with the development of cognitive and intellectual abilities. Among highly intelligent children and adolescents, cortical thinning started later but was more rapid (Shaw et al., 2006). In a study by Schnack and colleagues (2015), highly intelligent young adults had an accelerated rate of cortical thinning, which eventually reversed itself so that by the age of 42, a positive association was observed between total cortical thickness and intelligence. They suggest that cortical reduction increases the efficiency of the brain; and once optimum efficiency is reached, local connections are strengthened via cortical thickening.

This may explain the mixed results previously observed between cortical thickness and intelligence. In children and adolescents, both positive (Karama et al., 2009; Karama et al., 2011), and negative (Squeglia, Jacobus, Sorg, Jernigan, & Tapert, 2013; Tamnes et al., 2011) associations between cortical thickness and intelligence have been observed. In young adults (mean age 19.9), volume and surface area were positively associated with intelligence, though cortical thickness was not (Colom et al., 2013). Similarly, another study of young adults (< 30) showed that cortical thickness had a non-significant negative association with intelligence (Tamnes et al., 2011). On the other hand, Narr et al. (2007) observed a positive correlation between intelligence and cortical thickness in a study including participants up to 44 years of age.

Given the age of the current sample (17 – 46 years), it was possible that the interaction between subject weights for C20 and *g* was due to accelerated cortical thinning in the younger participants. We implemented a post-hoc GLM to test this possibility. However, the interaction term age by *g* did not significantly predict variance in C20. Therefore, the relationship between C20 and *g* is unlikely to be due to interactions between cortical development and cognitive development. Although it is not clear why lower cortical grey

matter was observed in the current component, the present findings do not necessarily imply that *g* is associated with overall lower cortical volume or thickness. One study showed cortical thickness to be more associated with crystallized intelligence than fluid intelligence (Choi et al., 2008), and crystallized intelligence may be associated with a different component in the current study. Furthermore, the magnitude of cortical volume loss and thinning was not assessed. Since C48 is associated with greater surface area expansion, *g* may still be associated with overall greater cortical volume.

Neural efficiency hypothesis. Although C20 was not associated with greater cortical volume or thickness, the component was associated with higher FA in the right supramarginal gyrus, left postcentral gyrus, and left precuneus. The supramarginal gyrus integrates sensory information from multiple sensory modalities, and is important for language processing (Binder et al., 1997). The precuneus is involved in processing salient stimuli (Corbetta & Shulman, 2002), self-consciousness (Lou et al., 1999), visuospatial imagery (Fletcher et al., 1995), and episodic memory (Krause et al., 1999). The postcentral gyrus is the location of the primary somatosensory cortex. All these cortical regions are considered to be "hubs" which connect several other regions. For instance, the supramarginal gyrus and precuneus are important hubs in the default mode network (Greicius, Krasnow, Reiss, & Menon, 2003; Raichle et al., 2001), and the postcentral gyrus is a hub in the somatosensory network (Biswal, Yetkin, Haughton, & Hyde, 1995; Tomasi & Volkow, 2011). Thus, these regions are important for functional connectivity in the brain.

The supramarginal gyrus, postcentral gyrus, and precuneus may also play a role in promoting efficiency. Human intelligence has recently been approached through the use of graph theory to map the "small-world" topology of the brain. According to this paradigm, human brains are considered to have "small-world" properties, such as a few highly-connected hubs, short path length, and high local clustering. These properties promote global efficiency of the brain (Achard & Bullmore, 2007; Bullmore & Sporns, 2012), and appear to depend on the integrity of the white matter tracts (van den Heuvel & Sporns, 2011). One resting-state functional magnetic resonance imaging (fMRI) study employed graph theoretical methods to study *g* (van den Heuvel, Stam, Kahn, & Hulshoff Pol, 2009). The authors found that the path length in the precuneus, supramarginal gyrus, and medial prefrontal gyrus were inversely associated with intelligence. In other words, when these hubs were more directly connected to other regions in the brain, this was associated with higher *g*. One of the few structural studies assessing neural efficiency and *g*, measured path length in terms of the

number of fibre bundles in different cortical nodes (Li et al., 2009). Li and colleagues found a negative association between intelligence and path length in several hubs. The greatest association between path length and intelligence was observed in the left postcentral gyrus, but significant associations were also observed in the precuneus. This is directly comparable to the current study, where higher FA was observed in the left postcentral gyrus, left precuneus, and right supramarginal gyrus. Thus, both the studies by van den Heuvel and colleagues (2009) and Li and colleagues (2009) show that the precuneus, supramarginal gyrus, and postcentral gyrus may be important for promoting efficiency, and that this mediates intelligence. The relationship between functional efficiency and brain structure is not entirely understood (Bullmore & Sporns, 2009). However, the present results suggest that efficiency might be expressed in terms of the integrity of major tracts and the white matter integrity directly underlying certain hub regions, rather than their volume or cortical thickness.

Graph theory is a relatively new approach to neural efficiency. Earlier studies of neural efficiency show that intelligent people activate fewer brain areas and use less energy during problem solving, whilst less intelligent people tend to use broader areas and more energy (e.g. Doppelmayr, Klimesch, Stadler, Poellhuber, & Heine, 2002; Haier et al., 1988; Neubauer, Grabner, Freudenthaler, Beckmann, & Guthke, 2004; Reichle, Carpenter, & Just, 2000). However, other studies have demonstrated that intelligent people use more energy when performing extremely difficult tasks that less intelligent people appear to have "given up" on (Doppelmayr, Klimesch, Hödlmoser, Sauseng, & Gruber, 2005; Larson, Haier, LaCasse, & Hazen, 1995). In a study by Tang and colleagues (2010), BOLD signal in the right prefrontal and right parietal cortices was associated with *g* and performance on an n-back task. Furthermore, *g* was positively associated with the integrity of the white-matter tracts connecting these areas. Intriguingly, the association between BOLD-activation in these cortical regions and *g* was negative, so that more intelligent people used *less* energy. Thus, there appears to be an association between lower energy expenditure in cortical regions, and higher integrity in underlying white matter structures. In light of these studies, the lower volume and cortical thickness in the current component may reflect the tendency to expend less energy and to use narrower areas during problem-solving. Yet at this stage, such a link can only be speculative, and more experimental testing of this hypothesis would be necessary before such a link can be acknowledged.

Regional Expansions in Cortical Surface Area (C48)

In C48, surface area expansion was observed in a circumscribed set of areas within the frontal, parietal, temporal, and occipital regions, similar to those outlined in the P-FIT. It has been suggested that the P-FIT regions are functionally dependent on association tracts (Gläscher et al., 2010; Jung & Haier, 2007). However, the current component was associated with white matter integrity differences in commissural tracts. Thus, in neither the present component nor C20, was integrity in association tracts related to a bigger cortex. As expected, clusters in C48 included the bilateral frontal poles and right inferior frontal gyrus (including Broca's areas), bilateral posterior supramarginal gyri (BA 40 and 22; overlapping the superior temporal gyrus), the left DLPFC, and the left precentral gyrus. Additionally, the right lateral occipital cortex and the right middle temporal and inferior temporal gyrus were observed in the present component. However, contrary to expectations, the superior parietal cortex and somatosensory cortices were not present in the current component and the bilateral middle frontal gyri showed a decrease in surface area.

Previous studies show that intelligence is associated with cortical surface area expansion in the middle frontal gyrus (BA 46; Colom et al., 2013); the cingulate cortex, superior temporal gyrus, medial temporal lobe, fusiform gyrus, insula, orbitofrontal cortex, the left central sulcus, and lingual gyrus (Fjell et al., 2013); and the DLPFC (Román et al., 2014). In contrast to the findings of Colom and colleagues (2013) and our own expectations, the surface area in the bilateral middle frontal gyri (BA 46) decreased in the present component. However, we did observe surface area increase in the DLPFC, as observed by Román and colleagues (2014); as well as the inferior temporal gyrus and right lateral occipital cortex (adjacent to the fusiform gyrus), the left precentral gyrus (adjacent to the left central sulcus), and regions overlapping the orbitofrontal cortex as observed by Fjell et al. (2013).

Language ability appears to be associated with several of the regions in C48. The frontal poles and ventrolateral prefrontal cortex are associated with language production and comprehension (e.g. Caplan, 2006) as well as abstract thought (Badre, 2008; Badre & Wagner, 2007). The supramarginal and angular gyrus are involved in multisensory integration and language (Arslan, 2014). C48 also appears to be associated with visuospatial processing. Higher FA was observed in the corpus callosum, parahippocampal gyrus, inferior temporal gyrus, and corticospinal tract. Lower MD was observed in the lingual gyrus. The corpus callossum and lingual gyrus are both associated with spatial ability (Fornari, Knyazeva, Meuli, & Maeder, 2007; Hutchinson et al., 2009). Furthermore, the parahippocampal gyrus is

important for spatial navigation and memory (Hafting, Fyhn, Molden, Moser, & Moser, 2005). The inferior temporal gyrus and inferior parietal cortex are both part of the occipitotemporal pathways for visual processing (i.e. the "what" and "where" pathways; Mishkin, Ungerleider, & Macko, 1983). Thus, regions associated with both verbal and visuospatial ability are present in the component. This is not surprising, given how *g* loads directly on to the second-stratum verbal, perceptual, and image rotation abilities (Major, Johnson, & Deary, 2012)

Thus, the areas outlined by the P-FIT and previous lesion studies was mainly observed in the cortical surface modality. This may reflect the fact that the association between *g* and volume is largely mediated by surface area (Vuoksimaa et al., 2014). Regional surface area growth is proposed to be due to intracortical myelin growth which stretches the cortex (Seldon, 2005). Such a process is suggested to increase functional specialization, allow the affected cortices to better differentiate afferent signals, and to disentangle adjacent neuronal columns (Seldon, 2007). However, this process has been proposed to thin the cortex: since a negative association has been observed between cortical surface area and cortical thickness within the same regions (Hogstrom et al., 2012). This process may well explain the concomitant volumetric decline observed in several of the left-lateralized regions where bilateral surface area expansions were observed in C48 (i.e. the supramarginal gyrus, precentral gyrus, frontal pole, and inferior and middle frontal gyrus). Indeed, Hogstrom and colleagues observed the strongest associations between surface area expansion and cortical thinning in regions such as the middle frontal gyrus and the orbitofrontal cortex, which overlap regions where we observed concomitant volume decrease and area expansion. However, it is not clear why this mechanism was reflected in lower VBM rather than lower cortical thickness.

There was no significant association between FSIQ and C48. Thus, it appears that C48 is uniquely associated with *g*, when compared to FSIQ. Since *g* and FSIQ are highly correlated, we investigated whether C48 was differentially associated with high and low FSIQ. The participants were split by median FSIQ. High FSIQ showed a non-significant positive association with subject weights on C48, whereas low FSIQ showed a non-significant negative association. The correlation coefficients were significantly different, so this may indicate that C48 subject weights are insensitive to lower-range FSIQ. It is possible that since *g* is comprised of many different cognitive tests, it is more sensitive to the lower range of mental ability.

Multiple Structures underlying *g*

Individually, none of the significant components explained more than 3% of variance in *g*; and together, the three significant components only explained 6%. When all 34 components were included however, this explained 18.4% of variance in *g*. A recent SEM study of *g* modelled the variables total brain volume, cortical thickness, white matter structure, white matter hyperintensity load, iron deposits, and microbleeds. As in our study, all variables together explained 18.4% of the variance in *g* (Ritchie et al., 2015). Although this equivalence is likely to be a coincidence, this may indicate the approximate amount of variance in *g* which can be explained by neurobiological structure.

Our observation that multiple components were associated with *g* confirm findings made by Kievit et al. (2012); namely that eight or more components predicted *g* better than one or two multimodal components. Since Linked ICA reflects neurobiological components of variance in the brain, some of these components are expected to be associated with different cognitive processes. The current findings therefore support the mutualism theory (Van Der Maas et al., 2006); which predicts that a large number of cognitive processes covary during development, producing positive manifold, though this is not due to any single underlying cognitive trait or ability. Processing speed is suggested to affect other cognitive abilities and lead to positive manifold. Although one of the components, C8, was homologous to the predicted structure for processing speed; the effect size (R^2 = .018) between C8 and *g* was not greater than for the other significant components. The low effect size is somewhat surprising, considering the moderate correlation between processing speed and *g* (*r* = -.44 to -.52; Jensen 1998, p. 234). However, it is possible that other white matter indices predict processing speed better (see Future Directions). Taken together, the current findings strongly suggest that there is not a singular underlying biological structure for *g*, but several.

The Validity of using Linked ICA to study *g*

It is not unusual for complex traits to be influenced by several biological variables; as observed in ageing (Buckner, 2004), depression (aan het Rot, Mathew, & Charney, 2009), and schizophrenia (Ross, Margolis, Reading, Pletnikov, & Coyle, 2006). In the present case, *g* also appears to be influenced by a number of neurobiological components, each explaining a small proportion of variance. None of the components in the study survived correction for multiple comparisons. However, none of the components individually explained more than

3% of variance in *g*. This is comparable to genome-wide association studies (GWAS), where many single nucleotide polymorphisms (SNPs) explain a high proportion of variance, but frequently no single SNP survives corrections for multiple comparisons. Since this was an exploratory study which employed a novel method to uncover the multimodal structure underlying *g*, all nominally significant components were retained for further analysis. This also allows the data from the current study to be compared to future studies of *g* employing Linked ICA.

Limitations

The current study did not investigate the existence of gender differences in the biological basis of *g*. Although males and females are similar with regards to intelligence (Dykiert, Gale, & Deary, 2009), there appears to be differences in how this is reflected in brain morphometry, especially in children (Clayden et al., 2011; Schmithorst, 2009). In the current study, a near-significant gender by *g* interaction was observed for C8, showing that the component subject weighting was more predictive of *g* for women than for men. These findings appear to support those by Haier, Jung, Yeo, Head, and Alkire (2005), showing that more white matter areas were related to intelligence in women. We also observed higher subject weights for C20 among men; without further inquiry as to why this might be. Given these findings, future studies may want to conduct separate analyses for each gender.

Another issue is that there is no objective measure of which tests to include in *g*. Although *g*s based on different tests are highly correlated in psychometric terms (Johnson et al., 2008), a structural MRI study showed that different *g*s from different samples were associated with only partly overlapping cortical regions (Haier et al., 2009). Haier and colleagues therefore suggest that three or more tests should be included per group factor. Although multiple tests of intelligence and working memory were included in the current study, only two measures of attention were included.

The participants had an average IQ of 112.77. Studies show that people have different developmental trajectories of brain structure depending on their intelligence levels (Schnack et al., 2015; Shaw et al., 2006). Furthermore, intelligent individuals tend to employ parietal regions to a significantly larger extent (Gray, Chabris, & Braver, 2003; Langer et al., 2012; Lee et al., 2006). Thus, there is no guarantee that the components are equally sensitive to differences in *g* across all strata of intelligence. Blair (2007) has emphasized the need to distinguish between conceptions of intelligence as the most difficult thought processes of

highly intelligent individuals, and the processes that underlie behaviour common to everyone. The current results may therefore reflect processes which are more specific to people of higher intelligence. Since we analysed the components where a main effect was observed between *g* and the component subject weights, we did not further assess whether the components were differentially associated with high and low *g*. However, high and low FSIQ appeared to be differentially associated with subject weights on C48. The current study did not have the power to elucidate the exact nature of this association, but future studies may consider increasing the number of participants and grouping them after different levels of *g*.

In order to account for non-linear morphometric age trajectories (Moseley, 2002; Westlye et al., 2009), we corrected the associations between the *g* and the components' subject weights for linear and quadratic age effects. However, both the timing of brain changes, direction of change, as well as the velocity of change, may be important indicators of intelligence (Schnack et al., 2015; Shaw et al., 2006). During the early 40s, intelligent people may grow thicker cortices, whereas the brains of less intelligent people remain stable or shrink. At this age, the velocity of growth was better able to predict intelligence than absolute levels of cortical thickness (Schnack et al., 2015). Thus, a cross-sectional study may not be adequate to capture intelligence phenotypes reflected in the velocity or timing of cortical change. The current study aimed to capture intelligence structures indifferent to age, and no age by *g* interaction was observed for C20. However, we cannot rule out that subtle interactions between *g* and age are not present in the current components. A longitudinal study would be better able to capture any such effects (e.g. Ramsden et al., 2011).

Future Directions

As noted above, relatively low effect sizes were observed between C8 subject weights and *g*. Alternative measures of white matter microstructure may be more sensitive neurobiological markers of *g* than the ones currently implemented. For instance, Penke and colleagues (2012) found that global longitudinal relaxation time (T1), a biomarker of white matter integrity reflecting brain tissue water content (Bastin, Sinha, Whittle, & Wardlaw, 2002), explained higher variance in *g* than global FA. Similarly, Ritchie and colleagues (2015) found that white matter hyperintensity load, explained unique variance in *g* when included together with global volume and cortical thickness, and that in this model global FA lost statistical significance. White matter hyperintensities are bright areas on a T2-weighted MRI image, and are associated with ageing, pathology, and cognitive deficits (Hernández et al., 2013). One study showed that hyperintensity load was more predictive of cognitive

functioning than regional FA in the elderly (Meier et al., 2012). However, it is not certain that these effects can be generalized to a younger sample.

One of the current study's major findings is that a large number of non-significant components were nevertheless able to describe a large portion of variance in *g*. We limited ourselves to describing the components which were nominally associated with *g*. However, some of these non-significant components were likely more predictive of *g* than others, and should be explored in greater detail.

A challenge of studying the cognitive underpinnings of *g* is that isolated cognitive abilities are difficult to measure (Bartholomew et al., 2009; Thomson, 1939) and prone to error (Schmiedek et al., 2014). For this reason, we selected a neurobiological approach to *g*. Nonetheless, the independent components may be associated with different cognitive processes. As such, a closer investigation into the cognitive underpinnings of these components may also inform our understanding of *g*. For instance, future studies may consider investigating whether the association between C8 and *g* is mediated by processing speed; by including measures of visual inspection time. Similarly, we suggest that C20 may be associated with neural efficiency. This was however impossible to verify within the context of the study, and reflects the ongoing difficulties in reconciling the structural-based models of intelligence (e.g. P-FIT) and functional-based models (e.g. neural efficiency hypothesis). However, Linked ICA has the capacity to include both structural and functional modalities within the same analysis (e.g. Mueller et al., 2013). Neural efficiency is most directly assessed through functional neuroimaging methods (Neubauer & Fink, 2009), for instance by measuring BOLD fMRI activity (Reichle et al., 2000) or EEG alpha band power (Doppelmayr et al., 2002) during a task. Including fMRI or EEG measures alongside structural modalities may therefore elucidate whether the neurobiological structures are associated with efficiency.

Conclusion

We predicted that several components would be associated with *g*. Furthermore, the novel use of Linked ICA allowed us to explore the multimodal underpinnings of these expected components. We observed a component of global white matter integrity, of localized white matter integrity, and of cortical surface area expansion in a subset of regions. Several unique findings were made. Higher integrity in the major white matter tracts was associated with a decrease in cortical thickness and volume, as observed in C20. The component of

regional cortical surface expansion (C48) was associated with white matter integrity in the commissural tracts. Thus, no relationship was observed between greater cortical size and integrity in the association tracts. However, higher cortical FA in hub regions was associated with the integrity of the white matter tracts in C20, which we suggest may reflect neural efficiency. Finally, *g* was not associated with just one single component. This strongly suggests that *g* is not unitary at the neurobiological level. All components combined explained a large proportion of variance in *g*. Thus, *g* appears to be a multicomponent construct at the neurobiological level.

References

aan het Rot, M., Mathew, S. J., & Charney, D. S. (2009). Neurobiological mechanisms in major depressive disorder. *Canadian Medical Association Journal, 180*(3), 305-313. doi: 10.1503/cmaj.080697

Achard, S., & Bullmore, E. (2007). Efficiency and cost of economical brain functional networks. *PLoS Comput Biol, 3*(2), e17. doi: 10.1371/journal.pcbi.0030017

Ackerman, P. L., Beier, M. E., & Boyle, M. O. (2005). Working memory and intelligence: The same or different constructs? *Psychological Bulletin, 131*(1), 30. doi: 10.1037/0033-2909.131.1.30

Albo, Z., Di Prisco, G. V., & Vertes, R. P. (2011). Multisite Spike-Field Coherence, Theta Rhythmicity, and Information Flow Within Papez's Circuit *Electrophysiological Recording Techniques* (pp. 191-213): Springer.

Ardila, A., Pineda, D., & Rosselli, M. (2000). Correlation between intelligence test scores and executive function measures. *Archives of Clinical Neuropsychology, 15*(1), 31-36. doi: 10.1016/S0887-6177(98)00159-0

Arslan, O. E. (2014). *Neuroanatomical basis of clinical neurology*: CRC Press.

Baddeley, A., Lewis, V., & Vallar, G. (1984). Exploring the articulatory loop. *The Quarterly journal of experimental psychology, 36*(2), 233-252. doi: 10.1080/14640748408402157

Badre, D. (2008). Cognitive control, hierarchy, and the rostro–caudal organization of the frontal lobes. *Trends in Cognitive Sciences, 12*(5), 193-200. doi: 10.1016/j.tics.2008.02.004

Badre, D., & Wagner, A. D. (2007). Left ventrolateral prefrontal cortex and the cognitive control of memory. *Neuropsychologia, 45*(13), 2883-2901. doi: 10.1016/j.neuropsychologia.2007.06.015

Barbey, A. K., Colom, R., Solomon, J., Krueger, F., Forbes, C., & Grafman, J. (2012). An integrative architecture for general intelligence and executive function revealed by lesion mapping. *Brain*, aws021. doi: 10.1093/brain/aws021

Barr, W. B. (2003). Neuropsychological testing of high school athletes: Preliminary norms and test–retest indices. *Archives of Clinical Neuropsychology, 18*(1), 91-101. doi: 10.1016/S0887-6177(01)00185-8

Bartholomew, D. J., Deary, I. J., & Lawn, M. (2009). A new lease of life for Thomson's bonds model of intelligence. *Psychological review, 116*(3), 567. doi: 10.1037/a0016262

Basten, U., Hilger, K., & Fiebach, C. J. (2015). Where smart brains are different: A quantitative meta-analysis of functional and structural brain imaging studies on intelligence. *Intelligence, 51*, 10-27. doi: 10.1016/j.intell.2015.04.009

Bastin, M. E., Sinha, S., Whittle, I. R., & Wardlaw, J. M. (2002). Measurements of water diffusion and T1 values in peritumoural oedematous brain. *Neuroreport, 13*(10), 1335-1340. doi: 10.1097/00001756-200207190-00024

Batty, G. D., Deary, I. J., & Gottfredson, L. S. (2007). Premorbid (early life) IQ and later mortality risk: systematic review. *Annals of epidemiology, 17*(4), 278-288. doi: 10.1016/j.annepidem.2006.07.010

Beaulieu, C. (2002). The basis of anisotropic water diffusion in the nervous system–a technical review. *NMR in Biomedicine, 15*(7-8), 435-455. doi: 10.1002/nbm.782

Benedict, R. H. (1997). *Brief visuospatial memory test--revised: professional manual*: PAR.

Benjamini, Y., & Hochberg, Y. (1995). Controlling the false discovery rate: a practical and powerful approach to multiple testing. *Journal of the Royal Statistical Society. Series B (Methodological)*, 289-300.

Binder, J. R., Frost, J. A., Hammeke, T. A., Cox, R. W., Rao, S. M., & Prieto, T. (1997). Human brain language areas identified by functional magnetic resonance imaging. *The Journal of Neuroscience, 17*(1), 353-362.

Bishop, C. M. (1999). Variational principal components. doi: 10.1049/cp:19991160

Biswal, B., Yetkin, F. Z., Haughton, V. M., & Hyde, J. S. (1995). Functional connectivity in the motor cortex of resting human brain using echo-planar MRI. *Magnetic Resonance in Medicine, 34*(4), 537-541. doi: 10.1002/mrm.1910340409

Blair, C. (2007). Inherent limits on the identification of a neural basis for general intelligence. *Behavioral and Brain Sciences, 30*(02), 154-155. doi: 10.1017/S0140525X07001197

Bloom, J. S., & Hynd, G. W. (2005). The role of the corpus callosum in interhemispheric transfer of information: excitation or inhibition? *Neuropsychology review, 15*(2), 59-71. doi: 10.1007/s11065-005-6252-y

Bosnes, O. (2009). Norsk versjon av Wechsler Abbreviated Scale of Intelligence: Hvor godt er samsvaret mellom WASI og norsk versjon av Wechsler Adult Intelligence Scale-III?[The Norwegian version of Wechsler Abbreviated Scale of Intelligence (WASI):

Do scores on the WASI correspond with scores on the Norwegian version of the Wechsle Adult Intelligence Scale-III (WAIS-III)?]. *Tidsskrift for Norsk Psykologforening, 46*, 564-568.

Brandt, J., & Benedict, R. H. (2001). *Hopkins verbal learning test--revised: professional manual*: Psychological Assessment Resources.

Buckner, R. L. (2004). Memory and executive function in aging and AD: multiple factors that cause decline and reserve factors that compensate. *Neuron, 44*(1), 195-208. doi: 10.1016/j.neuron.2004.09.006

Bullmore, E., & Sporns, O. (2009). Complex brain networks: graph theoretical analysis of structural and functional systems. *Nature Reviews Neuroscience, 10*(3), 186-198. doi: 10.1038/nrn2575

Bullmore, E., & Sporns, O. (2012). The economy of brain network organization. *Nature Reviews Neuroscience, 13*(5), 336-349. doi: 10.1038/nrn3214

Bush, G. (2011). Cingulate, Frontal, and Parietal Cortical Dysfunction in Attention-Deficit/Hyperactivity Disorder. *Biological Psychiatry, 69*(12), 1160-1167. doi: 10.1016/j.biopsych.2011.01.022

Caplan, D. (2006). Why is Broca's area involved in syntax? *Cortex, 42*(4), 469-471. doi: 10.1016/S0010-9452(08)70379-4

Carlson, J. S., & Wiedl, K. H. (1992). The dynamic assessment of intelligence *Interactive assessment* (pp. 167-186): Springer.

Carroll, J. B. (1993). *Human cognitive abilities: A survey of factor-analytic studies*: Cambridge University Press.

Catani, M., Howard, R. J., Pajevic, S., & Jones, D. K. (2002). Virtual in vivo interactive dissection of white matter fasciculi in the human brain. *Neuroimage, 17*(1), 77-94. doi: 10.1006/nimg.2002.1136

Chiang, M.-C., Barysheva, M., Lee, A. D., Madsen, S., Klunder, A. D., Toga, A. W., . . . Wright, M. J. (2008). Brain fiber architecture, genetics, and intelligence: a high angular resolution diffusion imaging (HARDI) study *Medical Image Computing and Computer-Assisted Intervention–MICCAI 2008* (pp. 1060-1067): Springer.

Choi, Y. Y., Shamosh, N. A., Cho, S. H., DeYoung, C. G., Lee, M. J., Lee, J. M., . . . Lee, K. H. (2008). Multiple bases of human intelligence revealed by cortical thickness and neural activation. *J Neurosci, 28*(41), 10323-10329. doi: 10.1523/JNEUROSCI.3259-08.2008

Choudrey, R. A., & Roberts, S. J. (2001). *Flexible Bayesian independent component analysis for blind source separation.* Paper presented at the Proc. Int. Conf. on Independent Component Analysis and Signal Separation (ICA2001).

Clayden, J. D., Jentschke, S., Muñoz, M., Cooper, J. M., Chadwick, M. J., Banks, T., . . . Vargha-Khadem, F. (2011). Normative development of white matter tracts: similarities and differences in relation to age, gender, and intelligence. *Cerebral Cortex*, bhr243. doi: 10.1093/cercor/bhr243

Colom, R. (2007). Intelligence? What intelligence? *Behavioral and Brain Sciences, 30*(02), 155-156. doi: 10.1017/S0140525X07001215

Colom, R., Abad, F. J., Garcıa, L. F., & Juan-Espinosa, M. (2002). Education, Wechsler's full scale IQ, and g. *Intelligence, 30*(5), 449-462. doi: 10.1016/S0160-2896(02)00122-8

Colom, R., Burgaleta, M., Román, F. J., Karama, S., Álvarez-Linera, J., Abad, F. J., . . . Haier, R. J. (2013). Neuroanatomic overlap between intelligence and cognitive factors: Morphometry methods provide support for the key role of the frontal lobes. *Neuroimage, 72*, 143-152. doi: 10.1016/j.neuroimage.2013.01.032

Colom, R., Haier, R. J., Head, K., Álvarez-Linera, J., Quiroga, M. Á., Shih, P. C., & Jung, R. E. (2009). Gray matter correlates of fluid, crystallized, and spatial intelligence: Testing the P-FIT model. *Intelligence, 37*(2), 124-135. doi: 10.1016/j.intell.2008.07.007

Colom, R., Karama, S., Jung, R. E., & Haier, R. J. (2010). Human intelligence and brain networks. *Dialogues in clinical neuroscience, 12*(4), 489.

Colom, R., Rebollo, I., Palacios, A., Juan-Espinosa, M., & Kyllonen, P. C. (2004). Working memory is (almost) perfectly predicted by g. *Intelligence, 32*(3), 277-296. doi: 10.1016/j.intell.2003.12.002

Comon, P. (1994). Independent component analysis, a new concept? *Signal processing, 36*(3), 287-314. doi: 10.1016/0165-1684(94)90029-9

Corbetta, M., & Shulman, G. L. (2002). Control of goal-directed and stimulus-driven attention in the brain. *Nature Reviews Neuroscience, 3*(3), 201-215. doi: 10.1038/nrn755

Cornblatt, B. A., Risch, N. J., Faris, G., Friedman, D., & Erlenmeyer-Kimling, L. (1988). The Continuous Performance Test, identical pairs version (CPT-IP): I. New findings about sustained attention in normal families. *Psychiatry Res, 26*(2), 223-238. doi: 10.1016/0165-1781(88)90076-5

Coyle, T. R., Pillow, D. R., Snyder, A. C., & Kochunov, P. (2011). Processing speed mediates the development of general intelligence (g) in adolescence. *Psychological Science, 22*(10), 1265-1269. doi: 10.1177/0956797611418243

Crawford, J. R., Sutherland, D., & Garthwaite, P. H. (2008). On the reliability and standard errors of measurement of contrast measures from the D-KEFS. *Journal of the International Neuropsychological Society, 14*(06), 1069-1073. doi: 10.1017/S1355617708081228

Dale, A. M., Fischl, B., & Sereno, M. I. (1999). Cortical surface-based analysis: I. Segmentation and surface reconstruction. *Neuroimage, 9*(2), 179-194. doi: 10.1006/nimg.1998.0395

Dale, A. M., & Sereno, M. I. (1993). Improved localizadon of cortical activity by combining EEG and MEG with MRI cortical surface reconstruction: a linear approach. *Journal of Cognitive Neuroscience, 5*(2), 162-176. doi: 10.1162/jocn.1993.5.2.162

Deary, I. J., Bastin, M., Pattie, A., Clayden, J., Whalley, L., Starr, J., & Wardlaw, J. (2006). White matter integrity and cognition in childhood and old age. *Neurology, 66*(4), 505-512. doi: 10.1212/01.wnl.0000199954.81900.e2

Deary, I. J., Caryl, P. G., Egan, V., & Wight, D. (1989). Visual and auditory inspection time: Their interrelationship and correlations with IQ in high ability subjects. *Personality and Individual Differences, 10*(5), 525-533. doi: 10.1016/0191-8869(89)90034-2

Deary, I. J., Penke, L., & Johnson, W. (2010). The neuroscience of human intelligence differences. *Nat Rev Neurosci, 11*(3), 201-211. doi: 10.1038/nrn2793

Deary, I. J., Strand, S., Smith, P., & Fernandes, C. (2007). Intelligence and educational achievement. *Intelligence, 35*(1), 13-21. doi: 10.1016/j.intell.2006.02.001

Delis, D., Kaplan, E., & Kramer, J. (2001). D-KEFS: examiners manual. *San Antonio: The Psychological Corporation*.

Doppelmayr, M., Klimesch, W., Hödlmoser, K., Sauseng, P., & Gruber, W. (2005). Intelligence related upper alpha desynchronization in a semantic memory task. *Brain Res Bull, 66*(2), 171-177. doi: 10.1016/j.brainresbull.2005.04.007

Doppelmayr, M., Klimesch, W., Stadler, W., Poellhuber, D., & Heine, C. (2002). EEG alpha power and intelligence. *Intelligence, 30*(3), 289-302. doi: 10.1016/S0160-2896(01)00101-5

Douaud, G., Groves, A. R., Tamnes, C. K., Westlye, L. T., Duff, E. P., Engvig, A., . . . Monsch, A. U. (2014). A common brain network links development, aging, and

vulnerability to disease. *Proceedings of the National Academy of Sciences, 111*(49), 17648-17653. doi: 10.1073/pnas.1410378111

Douaud, G., Jbabdi, S., Behrens, T. E. J., Menke, R. A., Gass, A., Monsch, A. U., . . . Smith, S. (2011). DTI measures in crossing-fibre areas: Increased diffusion anisotropy reveals early white matter alteration in MCI and mild Alzheimer's disease. *Neuroimage, 55*(3), 880-890. doi: 10.1016/j.neuroimage.2010.12.008

Douaud, G., Smith, S., Jenkinson, M., Behrens, T., Johansen-Berg, H., Vickers, J., . . . Matthews, P. M. (2007). Anatomically related grey and white matter abnormalities in adolescent-onset schizophrenia. *Brain, 130*(9), 2375-2386. doi: 10.1093/brain/awm184

Dykiert, D., Gale, C. R., & Deary, I. J. (2009). Are apparent sex differences in mean IQ scores created in part by sample restriction and increased male variance? *Intelligence, 37*(1), 42-47. doi: 10.1016/j.intell.2008.06.002

Ennis, D. B., & Kindlmann, G. (2006). Orthogonal tensor invariants and the analysis of diffusion tensor magnetic resonance images. *Magnetic Resonance in Medicine, 55*(1), 136-146. doi: 10.1002/mrm.20741

Fabrigar, L. R., Wegener, D. T., MacCallum, R. C., & Strahan, E. J. (1999). Evaluating the use of exploratory factor analysis in psychological research. *Psychological methods, 4*(3), 272. doi: 10.1037/1082-989X.4.3.272

Fischl, B., & Dale, A. M. (2000). Measuring the thickness of the human cerebral cortex from magnetic resonance images. *Proceedings of the National Academy of Sciences, 97*(20), 11050-11055. doi: 10.1073/pnas.200033797

Fischl, B., Salat, D. H., Busa, E., Albert, M., Dieterich, M., Haselgrove, C., . . . Klaveness, S. (2002). Whole brain segmentation: automated labeling of neuroanatomical structures in the human brain. *Neuron, 33*(3), 341-355. doi: 10.1016/S0896-6273(02)00569-X

Fjell, A. M., Westlye, L. T., Amlien, I., Tamnes, C. K., Grydeland, H., Engvig, A., . . . Lundervold, A. (2013). High-expanding cortical regions in human development and evolution are related to higher intellectual abilities. *Cerebral Cortex*, bht201. doi: 10.1093/cercor/bht201

Fletcher, P., Frith, C., Baker, S., Shallice, T., Frackowiak, R., & Dolan, R. (1995). The mind's eye—precuneus activation in memory-related imagery. *Neuroimage, 2*(3), 195-200. doi: 10.1006/nimg.1995.1025

Fornari, E., Knyazeva, M. G., Meuli, R., & Maeder, P. (2007). Myelination shapes functional activity in the developing brain. *Neuroimage, 38*(3), 511-518. doi: 10.1016/j.neuroimage.2007.07.010

Fry, A. F., & Hale, S. (2000). Relationships among processing speed, working memory, and fluid intelligence in children. *Biological Psychology, 54*(1), 1-34. doi: 10.1016/S0301-0511(00)00051-X

Galton, F. (1869). *Hereditary genius*: Macmillan and Company.

Gignac, G. E. (2015). Raven's is not a pure measure of general intelligence: Implications for g factor theory and the brief measurement of g. *Intelligence, 52*, 71-79. doi: 10.1016/j.intell.2015.07.006

Gläscher, J., Rudrauf, D., Colom, R., Paul, L. K., Tranel, D., Damasio, H., & Adolphs, R. (2010). Distributed neural system for general intelligence revealed by lesion mapping. *Proc Natl Acad Sci U S A, 107*(10), 4705-4709. doi: 10.1073/pnas.0910397107

Gottfredson, L. S. (1997). Mainstream science on intelligence: An editorial with 52 signatories, history, and bibliography. *Intelligence, 24*(1), 13-23. doi: 10.1016/S0160-2896(97)90011-8

Gray, J. R., Chabris, C. F., & Braver, T. S. (2003). Neural mechanisms of general fluid intelligence. *Nature neuroscience, 6*(3), 316-322. doi: 10.1038/nn1014

Greicius, M. D., Krasnow, B., Reiss, A. L., & Menon, V. (2003). Functional connectivity in the resting brain: A network analysis of the default mode hypothesis. *Proceedings of the National Academy of Sciences of the United States of America, 100*(1), 253-258. doi: 10.1073/pnas.0135058100

Groves, A. R., Beckmann, C. F., Smith, S. M., & Woolrich, M. W. (2011). Linked independent component analysis for multimodal data fusion. *Neuroimage, 54*(3), 2198-2217. doi: 10.1016/j.neuroimage.2010.09.073

Groves, A. R., Smith, S. M., Fjell, A. M., Tamnes, C. K., Walhovd, K. B., Douaud, G., . . . Westlye, L. T. (2012). Benefits of multi-modal fusion analysis on a large-scale dataset: life-span patterns of inter-subject variability in cortical morphometry and white matter microstructure. *Neuroimage, 63*(1), 365-380. doi: 10.1016/j.neuroimage.2012.06.038

Hafting, T., Fyhn, M., Molden, S., Moser, M.-B., & Moser, E. I. (2005). Microstructure of a spatial map in the entorhinal cortex. *Nature, 436*(7052), 801-806. doi: 10.1038/nature03721

Haier, R. J., Colom, R., Schroeder, D. H., Condon, C. A., Tang, C., Eaves, E., & Head, K. (2009). Gray matter and intelligence factors: Is there a neuro-g? *Intelligence, 37*(2), 136-144. doi: 10.1016/j.intell.2008.10.011

Haier, R. J., Jung, R. E., Yeo, R. A., Head, K., & Alkire, M. T. (2005). The neuroanatomy of general intelligence: sex matters. *Neuroimage, 25*(1), 320-327. doi: 10.1016/j.neuroimage.2004.11.019

Haier, R. J., Siegel, B. V., Nuechterlein, K. H., Hazlett, E., Wu, J. C., Paek, J., . . . Buchsbaum, M. S. (1988). Cortical glucose metabolic rate correlates of abstract reasoning and attention studied with positron emission tomography. *Intelligence, 12*(2), 199-217. doi: 10.1016/0160-2896(88)90016-5

Helms-Lorenz, M., Van de Vijver, F. J., & Poortinga, Y. H. (2003). Cross-cultural differences in cognitive performance and Spearman's hypothesis: g or c? *Intelligence, 31*(1), 9-29. doi: 10.1016/S0160-2896(02)00111-3

Hernández, M. d. C. V., Booth, T., Murray, C., Gow, A. J., Penke, L., Morris, Z., . . . Bastin, M. E. (2013). Brain white matter damage in aging and cognitive ability in youth and older age. *Neurobiology of aging, 34*(12), 2740-2747. doi: 10.1016/j.neurobiolaging.2013.05.032

Hogstrom, L. J., Westlye, L. T., Walhovd, K. B., & Fjell, A. M. (2012). The structure of the cerebral cortex across adult life: age-related patterns of surface area, thickness, and gyrification. *Cerebral Cortex*, bhs231. doi: 10.1093/cercor/bhs231

Hunt, E. (2010). *Human intelligence*: Cambridge University Press.

Hutcheson, G. D., & Sofroniou, N. (1999). *The multivariate social scientist: Introductory statistics using generalized linear models*: Sage.

Hutchinson, A., Mathias, J. L., Jacobson, B. L., Ruzic, L., Bond, A. N., & Banich, M. (2009). Relationship between intelligence and the size and composition of the corpus callosum. *Experimental Brain Research, 192*(3), 455-464. doi: 10.1007/s00221-008-1604-5

Huttenlocher, P. R. (1990). Morphometric study of human cerebral cortex development. *Neuropsychologia, 28*(6), 517-527. doi: 10.1016/0028-3932(90)90031-I

Huttenlocher, P. R., & Dabholkar, A. S. (1997). Regional differences in synaptogenesis in human cerebral cortex. *Journal of comparative Neurology, 387*(2), 167-178.

Irwing, P., Hamza, A., Khaleefa, O., & Lynn, R. (2008). Effects of Abacus training on the intelligence of Sudanese children. *Personality and Individual Differences, 45*(7), 694-696. doi: 10.1016/j.paid.2008.06.011

Itahashi, T., Yamada, T., Nakamura, M., Watanabe, H., Yamagata, B., Jimbo, D., . . . Kato, N. (2015). Linked alterations in gray and white matter morphology in adults with high-functioning autism spectrum disorder: A multimodal brain imaging study. *NeuroImage: Clinical, 7*, 155-169. doi: 10.1016/j.nicl.2014.11.019

Jensen, A. R. (1998). *The g factor: The science of mental ability*: Praeger Westport, CT.

Jensen, A. R., & Weng, L.-J. (1994). What is a good g? *Intelligence, 18*(3), 231-258. doi: 10.1016/0160-2896(94)90029-9

Johnson, W., & Bouchard, T. J. (2005). The structure of human intelligence: It is verbal, perceptual, and image rotation (VPR), not fluid and crystallized. *Intelligence, 33*(4), 393-416. doi: 10.1016/j.intell.2004.12.002

Johnson, W., Nijenhuis, J. t., & Bouchard Jr, T. J. (2008). Still just 1 *g*: Consistent results from five test batteries. *Intelligence, 36*(1), 81-95. doi: 10.1016/j.intell.2007.06.001

Jung, R. E., & Haier, R. J. (2007). The Parieto-Frontal Integration Theory (P-FIT) of intelligence: converging neuroimaging evidence. *Behavioral and Brain Sciences, 30*(02), 135-154. doi: 10.1017/S0140525X07001185

Just, M. A., & Carpenter, P. A. (1992). A capacity theory of comprehension: individual differences in working memory. *Psychological review, 99*(1), 122. doi: 10.1037/0033-295X.99.1.122

Kail, R., & Salthouse, T. A. (1994). Processing speed as a mental capacity. *Acta Psychol (Amst), 86*(2), 199-225. doi: 10.1016/0001-6918(94)90003-5

Karama, S., Ad-Dab'bagh, Y., Haier, R. J., Deary, I. J., Lyttelton, O., Lepage, C., & Evans, A. (2009). Positive association between cognitive ability and cortical thickness in a representative US sample of healthy 6 to 18 year-olds. *Intelligence, 37*(2), 145-155. doi: 10.1016/j.intell.2008.09.006

Karama, S., Colom, R., Johnson, W., Deary, I. J., Haier, R., Waber, D. P., . . . Evans, A. C. (2011). Cortical thickness correlates of specific cognitive performance accounted for by the general factor of intelligence in healthy children aged 6 to 18. *Neuroimage, 55*(4), 1443-1453. doi: 10.1016/j.neuroimage.2011.01.016

Keefe, R. S., Goldberg, T. E., Harvey, P. D., Gold, J. M., Poe, M. P., & Coughenour, L. (2004). The Brief Assessment of Cognition in Schizophrenia: reliability, sensitivity,

and comparison with a standard neurocognitive battery. *Schizophrenia research, 68*(2), 283-297. doi: 10.1016/j.schres.2003.09.011

Kern, R., Nuechterlein, K., Green, M., Baade, L., Fenton, W., Gold, J., . . . Seidman, L. (2008). The MATRICS Consensus Cognitive Battery, part 2: co-norming and standardization. *American Journal of Psychiatry, 165*(2), 214-220. doi: 10.1176/appi.ajp.2007.07010043

Kievit, R. A., van Rooijen, H., Wicherts, J. M., Waldorp, L. J., Kan, K.-J., Scholte, H. S., & Borsboom, D. (2012). Intelligence and the brain: A model-based approach. *Cognitive neuroscience, 3*(2), 89-97. doi: 10.1080/17588928.2011.628383

Kincses, Z. T., Hořínek, D., Szabó, N., Tóth, E., Csete, G., Štěpán-Buksakowska, I., . . . Vécsei, L. (2013). The Pattern of Diffusion Parameter Changes in Alzheimer's Disease, Identified by Means of Linked Independent Component Analysis. *Journal of Alzheimer's Disease, 36*(1), 119-128. doi: 10.3233/JAD-122431

Krause, B., Schmidt, D., Mottaghy, F., Taylor, J., Halsband, U., Herzog, H., . . . Müller-Gärtner, H.-W. (1999). Episodic retrieval activates the precuneus irrespective of the imagery content of word pair associates. *Brain, 122*(2), 255-263. doi: 10.1093/brain/122.2.255

Langer, N., Pedroni, A., Gianotti, L. R., Hänggi, J., Knoch, D., & Jäncke, L. (2012). Functional brain network efficiency predicts intelligence. *Human Brain Mapping, 33*(6), 1393-1406. doi: 10.1002/hbm.21297

Larson, G. E., Haier, R. J., LaCasse, L., & Hazen, K. (1995). Evaluation of a “mental effort” hypothesis for correlations between cortical metabolism and intelligence. *Intelligence, 21*(3), 267-278. doi: 10.1016/0160-2896(95)90017-9

Le Bihan, D. (2003). Looking into the functional architecture of the brain with diffusion MRI. *Nature Reviews Neuroscience, 4*(6), 469-480. doi: 10.1038/nrn1119

Lebel, C., & Beaulieu, C. (2011). Longitudinal development of human brain wiring continues from childhood into adulthood. *The Journal of Neuroscience, 31*(30), 10937-10947. doi: 10.1523/JNEUROSCI.5302-10.2011

Lee, K. H., Choi, Y. Y., Gray, J. R., Cho, S. H., Chae, J.-H., Lee, S., & Kim, K. (2006). Neural correlates of superior intelligence: stronger recruitment of posterior parietal cortex. *Neuroimage, 29*(2), 578-586. doi: 10.1016/j.neuroimage.2005.07.036

Lezak, M. D. (2004). *Neuropsychological assessment*: Oxford university press.

Li, Y., Liu, Y., Li, J., Qin, W., Li, K., Yu, C., & Jiang, T. (2009). Brain anatomical network and intelligence. *PLoS Comput Biol, 5*(5), e1000395. doi: 10.1371/journal.pcbi.1000395

Lippa, S. M., & Davis, R. N. (2010). Inhibition/switching is not necessarily harder than inhibition: An analysis of the D-KEFS color-word interference test. *Archives of Clinical Neuropsychology*, acq001. doi: 10.1093/arclin/acq001

Lo, A. H., Humphreys, M., Byrne, G. J., & Pachana, N. A. (2012). Test–retest reliability and practice effects of the Wechsler Memory Scale-III. *J Neuropsychol, 6*(2), 212-231. doi: 10.1111/j.1748-6653.2011.02023.x

Lou, H. C., Kjaer, T. W., Friberg, L., Wildschiodtz, G., Holm, S., & Nowak, M. (1999). A 15O-H2O PET study of meditation and the resting state of normal consciousness. *Human Brain Mapping, 7*(2), 98-105.

Major, J. T., Johnson, W., & Deary, I. J. (2012). Comparing models of intelligence in Project TALENT: The VPR model fits better than the CHC and extended Gf–Gc models. *Intelligence, 40*(6), 543-559. doi: 10.1016/j.intell.2012.07.006

Markowitsch, H. J. (2005). 10 The neuroanatomy of memory. *The effectiveness of rehabilitation for cognitive deficits*, 105. doi: 10.1093/acprof:oso/9780198526544.003.0010

McDaniel, M. A. (2005). Big-brained people are smarter: A meta-analysis of the relationship between in vivo brain volume and intelligence. *Intelligence, 33*(4), 337-346. doi: 10.1016/j.intell.2004.11.005

McGrew, K. S. (1997). Analysis of the major intelligence batteries according to a proposed comprehensive Gf-Gc framework.

Meier, I. B., Manly, J. J., Provenzano, F. A., Louie, K. S., Wasserman, B. T., Griffith, E. Y., . . . Brickman, A. M. (2012). White matter predictors of cognitive functioning in older adults. *Journal of the International Neuropsychological Society, 18*(03), 414-427. doi: 10.1017/S1355617712000227

Mishkin, M., Ungerleider, L. G., & Macko, K. A. (1983). Object vision and spatial vision: two cortical pathways. *Trends in Neurosciences, 6*, 414-417. doi: 10.1016/0166-2236(83)90190-X

Mohn, C., Sundet, K., & Rund, B. R. (2012). The norwegian standardization of the MATRICS (measurement and treatment research to improve cognition in

schizophrenia) consensus cognitive battery. *Journal of Clinical and Experimental Neuropsychology, 34*(6), 667-677. doi: 10.1080/13803395.2012.667792

Mohn, C., Sundet, K., & Rund, B. R. (2014). The relationship between IQ and performance on the MATRICS consensus cognitive battery. *Schizophrenia Research: Cognition, 1*(2), 96-100. doi: 10.1016/j.scog.2014.06.003

Mori, S., Oishi, K., Jiang, H., Jiang, L., Li, X., Akhter, K., . . . Woods, R. (2008). Stereotaxic white matter atlas based on diffusion tensor imaging in an ICBM template. *Neuroimage, 40*(2), 570-582. doi: 10.1016/j.neuroimage.2007.12.035

Moseley, M. (2002). Diffusion tensor imaging and aging–a review. *NMR in Biomedicine, 15*(7-8), 553-560. doi: 10.1002/nbm.785

Mueller, S., Keeser, D., Samson, A. C., Kirsch, V., Blautzik, J., Grothe, M., . . . Reiser, M. F. (2013). Convergent findings of altered functional and structural brain connectivity in individuals with high functioning autism: a multimodal MRI study. *Plos One, 8*(6), e67329.

Narr, K. L., Woods, R. P., Thompson, P. M., Szeszko, P., Robinson, D., Dimtcheva, T., . . . Bilder, R. M. (2007). Relationships between IQ and regional cortical gray matter thickness in healthy adults. *Cerebral Cortex, 17*(9), 2163-2171. doi: 10.1093/cercor/bhl125

Nelson, H. E., & Willison, J. (1991). *National Adult Reading Test (NART)*: Nfer-Nelson.

Neubauer, A. C., & Fink, A. (2009). Intelligence and neural efficiency. *Neuroscience & Biobehavioral Reviews, 33*(7), 1004-1023. doi: 10.1016/j.neubiorev.2009.04.001

Neubauer, A. C., Grabner, R. H., Freudenthaler, H. H., Beckmann, J. F., & Guthke, J. (2004). Intelligence and individual differences in becoming neurally efficient. *Acta Psychol (Amst), 116*(1), 55-74. doi: 10.1016/j.actpsy.2003.11.005

Nisbett, R. E., Aronson, J., Blair, C., Dickens, W., Flynn, J., Halpern, D. F., & Turkheimer, E. (2012). Intelligence: new findings and theoretical developments. *Am Psychol, 67*(2), 130-159. doi: 10.1037/a0026699

Nuechterlein, K., Green, M., Kern, R., Baade, L., Barch, D., Cohen, J., . . . Gold, J. (2008). The MATRICS Consensus Cognitive Battery, part 1: test selection, reliability, and validity. *American Journal of Psychiatry, 165*(2), 203-213. doi: 10.1176/appi.ajp.2007.07010042

Panizzon, M. S., Fennema-Notestine, C., Eyler, L. T., Jernigan, T. L., Prom-Wormley, E., Neale, M., . . . Franz, C. E. (2009). Distinct genetic influences on cortical surface area and cortical thickness. *Cerebral Cortex*, bhp026. doi: 10.1093/cercor/bhp026

Parent, A. (1996). *Carpenter's human neuroanatomy*: Williams & Wilkins.

Penke, L., Maniega, S. M., Bastin, M., Hernandez, M. V., Murray, C., Royle, N., . . . Deary, I. J. (2012). Brain white matter tract integrity as a neural foundation for general intelligence. *Mol Psychiatry, 17*(10), 1026-1030. doi: 10.1038/mp.2012.66

Penke, L., Maniega, S. M., Murray, C., Gow, A. J., Hernández, M. C. V., Clayden, J. D., . . . Deary, I. J. (2010). A general factor of brain white matter integrity predicts information processing speed in healthy older people. *The Journal of Neuroscience, 30*(22), 7569-7574. doi: 10.1523/JNEUROSCI.1553-10.2010

Raichle, M. E., MacLeod, A. M., Snyder, A. Z., Powers, W. J., Gusnard, D. A., & Shulman, G. L. (2001). A default mode of brain function. *Proceedings of the National Academy of Sciences, 98*(2), 676-682. doi: 10.1073/pnas.98.2.676

Ramsden, S., Richardson, F. M., Josse, G., Thomas, M. S., Ellis, C., Shakeshaft, C., . . . Price, C. J. (2011). Verbal and non-verbal intelligence changes in the teenage brain. *Nature, 479*(7371), 113-116. doi: 10.1038/nature10514

Raven, J. C., & Court, J. H. (1998). *Raven's progressive matrices and vocabulary scales*: Oxford Psychologists Press.

Reichle, E. D., Carpenter, P. A., & Just, M. A. (2000). The Neural Bases of Strategy and Skill in Sentence-Picture Verification. *Cognitive psychology, 40*(4), 261-295. doi: 10.1006/cogp.2000.0733

Ritchie, S. J., Booth, T., Hernández, M. d. C. V., Corley, J., Maniega, S. M., Gow, A. J., . . . Starr, J. M. (2015). Beyond a bigger brain: Multivariable structural brain imaging and intelligence. *Intelligence, 51*, 47-56. doi: 10.1016/j.intell.2015.05.001

Román, F. J., Abad, F. J., Escorial, S., Burgaleta, M., Martínez, K., Álvarez-Linera, J., . . . Colom, R. (2014). Reversed hierarchy in the brain for general and specific cognitive abilities: A morphometric analysis. *Human Brain Mapping, 35*(8), 3805-3818. doi: 10.1002/hbm.22438

Rose, S. A., Feldman, J. F., Jankowski, J. J., & Van Rossem, R. (2008). A cognitive cascade in infancy: Pathways from prematurity to later mental development. *Intelligence, 36*(4), 367-378. doi: 10.1016/j.intell.2007.07.003

Ross, C. A., Margolis, R. L., Reading, S. A., Pletnikov, M., & Coyle, J. T. (2006). Neurobiology of schizophrenia. *Neuron, 52*(1), 139-153. doi: 10.1016/j.neuron.2006.09.015

Roth, G., & Dicke, U. (2005). Evolution of the brain and intelligence. *Trends in Cognitive Sciences, 9*(5), 250-257. doi: 10.1016/j.tics.2005.03.005

Salthouse, T. A. (1994). The nature of the influence of speed on adult age differences in cognition. *Dev Psychol, 30*(2), 240. doi: 10.1037/0012-1649.30.2.240

Salthouse, T. A. (1996). The processing-speed theory of adult age differences in cognition. *Psychological review, 103*(3), 403. doi: 10.1037/0033-295X.103.3.403

Salthouse, T. A. (2000). Aging and measures of processing speed. *Biological Psychology, 54*(1), 35-54. doi: 10.1016/S0301-0511(00)00052-1

Sanabria-Diaz, G., Melie-García, L., Iturria-Medina, Y., Alemán-Gómez, Y., Hernández-González, G., Valdés-Urrutia, L., . . . Valdés-Sosa, P. (2010). Surface area and cortical thickness descriptors reveal different attributes of the structural human brain networks. *Neuroimage, 50*(4), 1497-1510. doi: 10.1016/j.neuroimage.2010.01.028

Schmiedek, F., Lövdén, M., & Lindenberger, U. (2014). A task is a task is a task: Putting complex span, n-back, and other working memory indicators in psychometric context. *Front Psychol, 5*. doi: 10.3389/fpsyg.2014.01475

Schmithorst, V. J. (2009). Developmental sex differences in the relation of neuroanatomical connectivity to intelligence. *Intelligence, 37*(2), 164-173. doi: 10.1016/j.intell.2008.07.001

Schmithorst, V. J., Wilke, M., Dardzinski, B. J., & Holland, S. K. (2005). Cognitive functions correlate with white matter architecture in a normal pediatric population: A diffusion tensor MRI study. *Human Brain Mapping, 26*(2), 139-147. doi: 10.1016/j.intell.2008.07.001

Schnack, H. G., van Haren, N. E., Brouwer, R. M., Evans, A., Durston, S., Boomsma, D. I., . . . Pol, H. E. H. (2015). Changes in thickness and surface area of the human cortex and their relationship with intelligence. *Cerebral Cortex, 25*(6), 1608-1617. doi: 10.1093/cercor/bht357

Seldon, H. L. (2005). Does brain white matter growth expand the cortex like a balloon? Hypothesis and consequences. *Laterality: Asymmetries of Body, Brain, and Cognition, 10*(1), 81-95. doi: 10.1080/13576500342000310

Seldon, H. L. (2007). Extended neocortical maturation time encompasses speciation, fatty acid and lateralization theories of the evolution of schizophrenia and creativity. *Medical hypotheses, 69*(5), 1085-1089. doi: 10.1016/j.mehy.2007.03.001

Shaw, P., Greenstein, D., Lerch, J., Clasen, L., Lenroot, R., Gogtay, N., . . . Giedd, J. (2006). Intellectual ability and cortical development in children and adolescents. *Nature, 440*(7084), 676-679. doi: 10.1038/nature04513

Siegler, R. S. (2005). Children's learning. *American Psychologist, 60*(8), 769. doi: 10.1037/0003-066X.60.8.769

Sliwinski, M., & Buschke, H. (1999). Cross-sectional and longitudinal relationships among age, cognition, and processing speed. *Psychology and aging, 14*(1), 18. doi: 10.1037/0882-7974.14.1.18

Smith, R. S., & Koles, Z. J. (1970). Myelinated nerve fibers: computed effect of myelin thickness on conduction velocity. *American Journal of Physiology--Legacy Content, 219*(5), 1256-1258.

Smith, S. M., Jenkinson, M., Johansen-Berg, H., Rueckert, D., Nichols, T. E., Mackay, C. E., . . . Matthews, P. M. (2006). Tract-based spatial statistics: voxelwise analysis of multi-subject diffusion data. *Neuroimage, 31*(4), 1487-1505. doi: 10.1016/j.neuroimage.2006.02.024

Smith, S. M., Jenkinson, M., Woolrich, M. W., Beckmann, C. F., Behrens, T. E., Johansen-Berg, H., . . . Flitney, D. E. (2004). Advances in functional and structural MR image analysis and implementation as FSL. *Neuroimage, 23*, S208-S219. doi: 10.1016/j.neuroimage.2004.07.051

Sowell, E. R., Thompson, P. M., Leonard, C. M., Welcome, S. E., Kan, E., & Toga, A. W. (2004). Longitudinal mapping of cortical thickness and brain growth in normal children. *The Journal of Neuroscience, 24*(38), 8223-8231. doi: 10.1523/JNEUROSCI.1798-04.2004

Spearman, C. (1904). "General Intelligence," objectively determined and measured. *The American Journal of Psychology, 15*(2), 201-292. doi: 10.2307/1412107

Spearman, C. (1927). The abilities of man.

Squeglia, L. M., Jacobus, J., Sorg, S. F., Jernigan, T. L., & Tapert, S. F. (2013). Early adolescent cortical thinning is related to better neuropsychological performance. *Journal of the International Neuropsychological Society, 19*(09), 962-970. doi: 10.1017/S1355617713000878

Strauss, E., Sherman, E. M., & Spreen, O. (2006). *A compendium of neuropsychological tests: Administration, norms, and commentary*: Oxford University Press.

Strenze, T. (2007). Intelligence and socioeconomic success: A meta-analytic review of longitudinal research. *Intelligence, 35*(5), 401-426. doi: 10.1016/j.intell.2006.09.004

Tamnes, C. K., Fjell, A. M., Østby, Y., Westlye, L. T., Due-Tønnessen, P., Bjørnerud, A., & Walhovd, K. B. (2011). The brain dynamics of intellectual development: Waxing and waning white and gray matter. *Neuropsychologia, 49*(13), 3605-3611. doi: 10.1016/j.neuropsychologia.2011.09.012

Tang, C. Y., Eaves, E. L., Ng, J. C., Carpenter, D. M., Mai, X., Schroeder, D. H., . . . Haier, R. J. (2010). Brain networks for working memory and factors of intelligence assessed in males and females with fMRI and DTI. *Intelligence, 38*(3), 293-303. doi: 10.1016/j.intell.2010.03.003

Thomson, G. (1939). The factorial analysis of human ability. *British Journal of Educational Psychology, 9*(2), 188-195. doi: 10.1111/j.2044-8279.1939.tb03204.x

Tomasi, D., & Volkow, N. D. (2011). Association between functional connectivity hubs and brain networks. *Cerebral Cortex, 21*(9), 2003-2013. doi: 10.1093/cercor/bhq268

Urbanski, M., De Schotten, M. T., Rodrigo, S., Catani, M., Oppenheim, C., Touzé, E., . . . Dubois, B. (2008). Brain networks of spatial awareness: evidence from diffusion tensor imaging tractography. *Journal of Neurology, Neurosurgery & Psychiatry, 79*(5), 598-601. doi: 10.1136/jnnp.2007.126276

van den Heuvel, M. P., & Sporns, O. (2011). Rich-club organization of the human connectome. *The Journal of Neuroscience, 31*(44), 15775-15786. doi: 10.1523/JNEUROSCI.3539-11.2011

van den Heuvel, M. P., Stam, C. J., Kahn, R. S., & Hulshoff Pol, H. E. (2009). Efficiency of functional brain networks and intellectual performance. *J Neurosci, 29*(23), 7619-7624. doi: 10.1523/JNEUROSCI.1443-09.2009

Van Der Maas, H. L., Dolan, C. V., Grasman, R. P., Wicherts, J. M., Huizenga, H. M., & Raijmakers, M. E. (2006). A dynamical model of general intelligence: the positive manifold of intelligence by mutualism. *Psychological review, 113*(4), 842. doi: 10.1037/0033-295X.113.4.842

Vaskinn, A., & Sundet, K. (2001). Estimating premorbid IQ: A Norwegian version of National Adult Reading Test. *J Nor Psychol Assoc, 38*, 1133-1140.

Vernon, P. E. (1965). Ability factors and environmental influences. *American Psychologist, 20*(9), 723. doi: 10.1037/h0021472

Vuoksimaa, E., Panizzon, M. S., Chen, C.-H., Fiecas, M., Eyler, L. T., Fennema-Notestine, C., . . . Jak, A. (2014). The genetic association between neocortical volume and general cognitive ability is driven by global surface area rather than thickness. *Cerebral Cortex*, bhu018.

Wakana, S., Jiang, H., Nagae-Poetscher, L. M., Van Zijl, P. C., & Mori, S. (2004). Fiber tract–based atlas of human white matter anatomy 1. *Radiology, 230*(1), 77-87. doi: 10.1148/radiol.2301021640

Walhovd, K. B., Fjell, A. M., Reinvang, I., Lundervold, A., Fischl, B., Salat, D., . . . Dale, A. M. (2005). Cortical volume and speed-of-processing are complementary in prediction of performance intelligence. *Neuropsychologia, 43*(5), 704-713. doi: 10.1016/j.neuropsychologia.2004.08.006

Waxman, S. G. (1980). Determinants of conduction velocity in myelinated nerve fibers. *Muscle & nerve, 3*(2), 141-150. doi: 10.1002/mus.880030207

Wechsler, D. (1997a). *WAIS-III: Administration and scoring manual: Wechsler adult intelligence scale*: Psychological Corporation.

Wechsler, D. (1997b). *Wechsler memory scale (WMS-III)*: Psychological Corporation.

Wechsler, D. (2007). Wechsler abbreviated scale of intelligence (WASI). Norwegian manual supplement. *Stockholm, Sweden: Harcourt Assessment*.

Westlye, L. T., Walhovd, K. B., Dale, A. M., Bjørnerud, A., Due-Tønnessen, P., Engvig, A., . . . Fjell, A. M. (2009). Life-span changes of the human brain white matter: diffusion tensor imaging (DTI) and volumetry. *Cerebral Cortex*. doi: 10.1093/cercor/bhp280

Wiens, A. N., Bryan, J. E., & Crossen, J. R. (1993). Estimating WAIS-R FSIQ from the national adult reading test-revised in normal subjects. *The Clinical Neuropsychologist, 7*(1), 70-84. doi: 10.1080/13854049308401889

Winkler, A. M., Kochunov, P., Blangero, J., Almasy, L., Zilles, K., Fox, P. T., . . . Glahn, D. C. (2010). Cortical thickness or grey matter volume? The importance of selecting the phenotype for imaging genetics studies. *Neuroimage, 53*(3), 1135-1146. doi: 10.1016/j.neuroimage.2009.12.028

Woods, S. P., Scott, J. C., Conover, E., Marcotte, T. D., Heaton, R. K., & Grant, I. (2005). Test-retest reliability of component process variables within the Hopkins Verbal Learning Test-Revised. *Assessment, 12*(1), 96-100. doi: 10.1177/1073191104270342

Woolrich, M. W., Jbabdi, S., Patenaude, B., Chappell, M., Makni, S., Behrens, T., . . . Smith, S. M. (2009). Bayesian analysis of neuroimaging data in FSL. *Neuroimage, 45*(1), S173-S186. doi: 10.1016/j.neuroimage.2008.10.055

Yu, C., Li, J., Liu, Y., Qin, W., Li, Y., Shu, N., . . . Li, K. (2008). White matter tract integrity and intelligence in patients with mental retardation and healthy adults. *Neuroimage, 40*(4), 1533-1541. doi: 10.1016/j.neuroimage.2008.01.063

Zatorre, R. J., Fields, R. D., & Johansen-Berg, H. (2012). Plasticity in gray and white: neuroimaging changes in brain structure during learning. *Nature neuroscience, 15*(4), 528-536. doi: 10.1038/nn.3045

Østby, Y., Tamnes, C. K., Fjell, A. M., Westlye, L. T., Due-Tønnessen, P., & Walhovd, K. B. (2009). Heterogeneity in Subcortical Brain Development: A Structural Magnetic Resonance Imaging Study of Brain Maturation from 8 to 30 Years. *The Journal of Neuroscience, 29*(38), 11772-11782. doi: 10.1523/jneurosci.1242-09.2009

Supplementary Information

Appendix A

Appendix A gives a description all the tests included in the study. Validity and reliability measures are included where available. Several of the tests were taken from the Norwegian Matrics Consensus Cognitive Battery (MCCB; Mohn, Sundet, & Rund, 2012). MCCB is a hybrid battery composed of multiple independent tests measuring cognitive ability. The tests are taken from other batteries, including the Wechsler Adult Intelligence Scale – Third Edition (WAIS-III; Wechsler, 1997a) and Wechsler's Memory Scale- Third Edition (WMS-III, Wechsler, 1997b). Although primarily used to measure cognitive impairment in psychotic disorders, the tests are standardized to a healthy population (Kern et al., 2008). The MCCB composite score of all tests is highly correlated with WAIS FSIQ in a Norwegian sample (r = .69) (Mohn, Sundet, & Rund, 2014). In order to appropriately sample higher-level intelligence, tests with strong ceiling effects (mode = maximum value) were excluded. When there were several related measures, only one test was included in order to ensure independence (Jensen & Weng, 1994).

Intelligence Tests

WASI IQ Tests. We employed the Norwegian version of the Wechsler Abbreviated Scale of Intelligence (Wechsler, 2007). The four subtests were Vocabulary, Similarities, Block Design, and Matrix Reasoning. In Vocabulary, the participant must correctly define a word. In Similarities, the participant must explain how two words are conceptually related. In Block Design, the participant must replicate with blocks a two-colour design. In Matrix Reasoning, the participant views a matrix with section missing and must identify the correct response option of five available. Vocabulary and Similarities indicate verbal intelligence (VIQ), and Block Design and Matrix Reasoning indicate perceptual intelligence (PIQ). Validity coefficients between the Norwegian WASI and WAIS-III are r = .86 for PIQ, r = .88 for VIQ, and r = .93 for FSIQ (Bosnes, 2009). The split-half reliability for WASI VIQ, PIQ, and FSIQ are .96, .96, and .98 (Strauss, Sherman, & Spreen, 2006).

NART. The Norwegian version (Vaskinn & Sundet, 2001) of the National Adult Reading Test (NART; Nelson & Willison, 1991) measures verbal ability, and is used to measure premorbid intellectual ability among clinical groups. The test comprises of 50 irregularly spelled words. For each word that the participant is familiar with, they must give what they believe to be the correct pronunciation. NART scores are given in number of errors, which are inversely coded. The correlation between NART and WAIS is r = .70-.80 (Lezak,

2004). In American samples, NART correlates with years of education and socioeconomic status, though not gender or ethnicity FSIQ (Wiens, Bryan, & Crossen, 1993).

Working Memory Tests

WAIS-III Digit Span. The Digit Span subtest measures auditory working memory, and is taken from WAIS-III. The participant repeats 3 – 9 digits in the forwards and 2 – 9 in the backwards order. The two tests are considered to measure slightly different constructs, as the forwards task loads on to short-term memory, whereas the backwards task also requires reordering and manipulation, thereby also measuring working memory. The backwards task was selected for inclusion in this study. Digit span had very high split-half reliability (> .90), and high test-retest reliability (.80 - .90; Strauss et al., 2006).

MCCB Letter-Number Span. The MCCB Letter-Number Span test measures auditory working memory. Participants are read a series of letters and numbers, and asked to recite them back in ascending order starting with numbers. Scores are given as the number of correctly managed trials.

MCCB WMS-III Logical Memory I. The MCCB Logical Memory I test is taken from the WMS-III, and measures auditory short-term memory. The participant hears two stories, and after each, gives a free recall. The number of specific story details and thematic details are noted in the recall. This study only used the story score since thematic score showed strong ceiling effects. Logical memory 1 has high (.80 – .89) internal consistency, and adequate test-retest reliability (.70 – .79; Strauss et al., 2006).

MCCB WMS-III Spatial Memory Sequencing. The Spatial Memory Sequencing test measures spatial short-term memory, and is taken from the WMS-III. There are 10 irregularly spaced cubes on a board. The experimenter taps the cubes in a certain order, and the participant must tap the cubes in either the same or the reverse order. Progressively, the trials become more difficult, as the sequences become longer. Although designed to be analogous to the auditory digit span, people score better in the backward spatial span than forwards spatial span. Therefore, the forwards test was used in the current study. The Spatial Memory Sequencing test has a modest test-retest reliability of .46 – .64 in an older population (Lo, Humphreys, Byrne, & Pachana, 2012).

MCCB BVMT-R. The MCCB Brief Visuospatial Memory Test-Revised (BVMT-R; Benedict, 1997) measures visual working memory as well as learning. The participant is shown a page with 6 geometric figures for 10 seconds, and must then reproduce the geometric

forms in the correct spatial location from memory. This is repeated two more times with the same configuration, giving the participant two more chances to perform correctly. This study utilized the sum of all three trials. Immediate recall test-retest reliability was .60 – .84, from trial 1 to trial 3 (Benedict, 1997).

MCCB HVLT-R. The MCCB Hopkins Verbal Learning Test – Revised (HVLT-R; Brandt & Benedict, 2001) measures short- and long-term verbal memory, although only the short-term condition was used here. The participant hears 12 nouns belonging to three different semantic categories, and has to recall as many words as they can. The same list of words is repeated over two more trials, and the participant gets a chance to recall more words. The sum-score of all three conditions was utilized here. Test-retest reliability for the HVLT-R is .49-.55 (Barr, 2003; Woods et al., 2005).

Attention Tests

MCCB CPT-IP. The MCCB Continuous Performance Test – Identical Pairs (CPT-IP; Cornblatt, Risch, Faris, Friedman, & Erlenmeyer-Kimling, 1988) is a variant of the Continuous Performance Test, and measures sustained attention and response inhibition. The participants are presented with a series of 2-4 digit codes, and must quickly press a button each time identical codes are presented in a row. The 4-digit condition measures attention and working memory. d' is the ability of participants to discriminate signal from background noise, and was calculated for each digit-condition, based on hits and false alarms. d' thus takes tendencies to either over- or under-respond into account. The 4-digit condition was included in the current study. Test-retest reliability for the d-prime across all digit conditions is.56 – .73 (Cornblatt et al., 1988).

D-KEFS CWIT. The D-KEFS Color-Word Interference Test (CWIT; Delis et al., 2001) is a Stroop test which measures cognitive processing speed and executive functioning; in particular inhibitory control and cognitive flexibility. There are two baseline trials; colour naming and word reading. After this there is an inhibition trial, where the subject must avoid reading the word and name the word's ink colour instead, and an inhibition/switching trial where participants switch between naming the ink colour and reading the word. This study included only the inhibition trial, since this was the trial which our sample found the most challenging. This was likely due to practice effects in the fourth trial (Lippa & Davis, 2010). Usually the baselines scores are subtracted from the inhibition scores. As we were not interested in removing the effect of baseline processing speed, and as the raw scores have

higher test-retest reliability than composite scores (Crawford, Sutherland, & Garthwaite, 2008), the current study utilized the raw scores of the inhibition trial. Test-retest reliability scores for raw scores of all conditions are .62-.76 (Delis et al., 2001).

Cognitive Processing Speed Tests

MCCB TMT Part A. Part A of the Trail Making Test (TMT) assesses cognitive processing speed, visual scanning, visuomotor tracking, and cognitive shifting. The participant must draw lines between numbers in ascending order, and the score is given as number of seconds. The inverted raw score was utilized. TMT moderately correlates with performance IQ in adolescents (r = -.31; Ardila, Pineda, & Rosselli, 2000).

MCCB BACS Symbol Coding. The symbol coding subtest from the Brief Assessment of Cognition in Schizophrenia (BACS; Keefe et al., 2004) tests measures working memory and cognitive processing speed. Symbol coding is a timed paper and pencil test in which the participant uses a key to decipher symbols into numerical digits. The task also measures working memory. Intraclass correlation for healthy controls was .83 (Keefe et al., 2004).

MCCB Word Fluency: Animal Naming. The Animal Naming test measures cognitive processing speed, inhibitory control, and verbal fluency. The participant must name as many animals as he or she can within a minute, and the raw score is given as the number of individual animals named.

Appendix B

Component 8

C8 was characterized by major clusters of global white matter microstructural changes in the MD (31648 voxels) modality, and the FA (8405 voxels) modality. The MD modality decreased in all the anatomical structures identified by the JHU ICBM-DTI-81 atlas in FSL. These included: **tracts in the brainstem** (corticospinal tract; medial lemniscus; inferior, middle, and superior cerebellar peduncle; pontine crossing path); **projection fibres** (anterior and superior corona radiata; anterior, retrolenticular, and posterior limb of the internal capsule; cerebral peduncle; posterior thalamic radiation; posterior thalamic radiation); **association fibres** (superior longitudinal fasciculus; superior fronto-occipital fasciculus; uncinate fasciculus; inferior fronto-occipital fasciculus / inferior longitudinal fasciculus; sagittal stratum; external capsule; cingulum; fornix; stria terminalis); and **commissural fibres** (anterior commissure; corpus callosum; tapetum) (all bilateral).

A concurrent increase in FA was observed in all of these same areas, except the middle cerebral peduncle, pontine crossing path, fornix, medial lemniscus, inferior cerebral peduncle, left superior cerebral peduncle, uncinate fasciculus, and left tapetum.

Component 20 and 48

C20 and C48 consisted of multiple clusters in each modality. The ten greatest clusters in each modality are represented in Table 6; showing the number of voxels in the cluster, an indication of whether increasing or decreasing values were observed (+ / -), the anatomical region at the peak intensity of the cluster, the MNI coordinates of the cluster peak, other anatomical regions in the cluster, and the Brodmann areas in the cluster peak.

The Harvard-Oxford Cortical Structural Atlas was used to identify grey matter regions in the arealization, cortical thickness, and VBM modalities. Within the FA, MD, and MO modalities, the JHU ICBM-DTI-81 White-Matter Label Atlas was used to classify white matter anatomical regions and the Harvard-Oxford Cortical Structural Atlas was used to identify cortical white matter associations.

Cluster descriptions for C20

Modality: Cortical thickness (6%)					
Voxels	*+ / -*	*Cluster peak*	*Other regions in cluster*	*MNI coordinates*	*Brodmann area*
872	-	R frontal orbital cortex	L frontal orbital cortex; L subcallosal cortex	16, 16, -20	11
633	-	L cingulate gyrus, anterior division		-4, 24, 18	unclassified
463	-	R insular cortex		38, -16, -4	48
399	-	L parahippocampal gyrus, anterior division	L temporal fusiform cortex	-60	35
304	-	R supramarginal gyrus, anterior division	R postcentral gyrus; R primary somatosensory cortex	58, -22, 30	48
226	-	L insular cortex		-48	48
51	-	R cingulate gyrus, anterior division		6, 32, 10	25
32	-	R inferior temporal gyrus, posterior division		56, -22, -24	20
28	-	R frontal pole		12, 48, -22	11
16	-	R parahippocampal gyrus, posterior division		26, -26, -14	20
3	-	R middle temporal gyrus, temporooccipital part		58, -48, -8	37

Modality: VBM (9%)					
Voxels	*+ / -*	*Cluster peak*	*Other regions in cluster*	*MNI coordinates*	*Brodmann area*
8582	-	R middle temporal gyrus, temperooccipital part	R frontal and temporal cortices; R supramarginal gyrus and angular gyrus; R lateral occipital cortex	62, -50, -8	37
2443	-	L middle temporal gyrus, posterior division	L temporal cortex; L postcentral gyrus; L supramarginal gyrus	-104	21
2038	-	L lingual gyrus	R lingual gyrus; callosal gyri; bilateral cingulate gyri; bilateral parahippocampal gyri	-10, -54, 0	18
728	-	cerebellum		42, -70, -36	
377	-	L superior temporal gyrus, anterior division	L postcentral gyrus; L middle temporal gyrus anterior division; L inferior temporal gyrus; L supramarginal gyrus; L central opercular cortex	-68	22
326	-	R occipital pole,	R lateral occipital cortex	22, -94, 20	18
250	-	R occipital pole,		18, -98, -12	18
145	-	R superior parietal lobule		10, -54, 68	5
133	-	L insular cortex		-34, 6, 0	48
38	-	L central opercular cortex		-42, -14, 12	48

Cluster descriptions for C20

Modality: FA (32%)					
Voxels	*+ / -*	*Cluster peak*	*Other regions in cluster*	*MNI coordinates*	*Brodmann area*
560	+	unclassified	R anterior corona radiata; R cingulum; L fornix; L internal capsule; L inferior fronto-occipital fasciculus / L inferior longitudinal fasciculus	12, 6, -6	
196	+	unclassified	L external capsule; L uncinate fasciculus	-26, 16, -8	
173	+	unclassified	L superior longitudinal fasciculus	-34, -50, 30	
162	+	R sagittal stratum (inferior longitudinal fasciculus and inferior fronto-occipital fasciculus)		38, -18, -8	
128	+	L postcentral gyrus		-32, -22, 40	
126	+	L precuneus cortex		-24, -50, 4	
82	+	unclassified		30, -36, 38	
78	+	fornix (column and body of fornix)		-2, -10, 16	
39	+	R inferior longitudinal fasciculus		46, -28, -14	
37	+	R supramarginal gyrus, posterior division		46, -42, 42	40

Cluster descriptions for C20

Modality: MO (31%)					
Voxels	*+ / -*	*Cluster peak*	*Other regions in cluster*	*MNI coordinates*	*Brodmann area*
182	+	L sagittal stratum (includes inferior longitudinal fasciculus and inferior fronto-occipital fasciculus)	L internal capsule	-64	
144	+	R sagittal stratum (includes inferior fronto-occipital fasciculus and inferior fronto-occipital fasciculus)		38, -16, -10	
90	+	unclassified		48, -26, -16	
71	-	unclassified		-16, -26, 56	
69	+	R superior longitudinal fasciculus		44, -12, 28	
47	-	L superior parietal lobule		-22, -44, 48	unclassified
46	+	unclassified		30, -42, 36	
37	+	unclassified		10, -20, 2	
36	+	L superior corona radiata		-26, -4, 20	
35	+	L superior longitudinal fasciculus		-44, -12, 26	

Cluster descriptions for C48

Modality: Area (7%)					
Voxels	*+ / -*	*Cluster peak*	*Other regions in cluster*	*MNI coordinates*	*Brodmann area*
950	+	R frontal pole	R inferior frontal gyrus, pars triangularis	44, 40, 4	45
332	+	L precentral gyrus; L inferior frontal gyrus, pars opercularis		-46, 6, 28	44
321	+	R middle temporal and inferior temporal gyrus, temporoccipital part		56, -46, -10	20
161	+	R supramarginal gyrus posterior division; R angular gyrus		56, -42, 40	40
150	-	R middle frontal gyrus		32, 34, 34	46
140	-	L middle frontal gyrus		-40, 36, 30	46
97	+	L middle frontal gyrus		-38, 10, 56	9
97	+	L supramarginal gyrus, posterior division		-52, -50, 28	22
65	+	R lateral occipital cortex, inferior division		40, -66, 14	37
35	+	L frontal pole		-38, 42, -2	47

Cluster descriptions for C48

Modality: VBM (6%)					
Voxels	*+ / -*	*Cluster peak*	*Other regions in cluster*	*MNI coordinates*	*Brodmann area*
2078	-	R precentral gyrus	L precentral gyrus, bilateral superior frontal gyrus	26, -18, 68	6
389	-	L frontal pole	L middle frontal gyrus	-26, 46, 32	46
322	-	L postcentral gyrus	L supramarginal gyrus	-66, -22, 20	22
296	+	L precuneus cortex	R precuneus cortex	-2, -62, 32	unclassified
81	-	L supramarginal gyrus, anterior division		-58, -34, 40	40
58	-	L inferior frontal gyrus, pars opercularis		-58, 10, 8	6
50	+	L occipital pole		-120	17
32	+	R temporal fusiform cortex, posterior division		26, -38, -24	37
24	-	L inferior frontal gyrus, pars opercularis	L middle frontal gyrus	-54, 18, 28	44
19	-	L angular gyrus		-46, -54, 20	39

Cluster descriptions for C48

Modality: FA (30%)					
Voxels	*+ / -*	*Cluster peak*	*Other regions in cluster*	*MNI coordinates*	*Brodmann area*
123	+	R corticospinal tract		6, -26, -36	
110	+	L body of corpus callosum	R body of corpus callosum	-4, -16, 26	
102	-	L corticospinal tract		-62	
51	-	R angular gyrus		42, -50, 40	40
48	+	R splenium of corpus callosum	L splenium of corpus callosum	2, -34, 16	unclassified
44	+	L parahippocampal gyrus, anterior division		-78	30
34	+	R inferior temporal gyrus, temporooccipital part		48, -52, -8	37
33	+	L precuneus cortex		-16, -58, 34	unclassified
29	+	L superior frontal gyrus		-16, 22, 42	32
24	+	L inferior temporal gyrus, temporooccipital part		-106	37

Cluster descriptions for C48

Modality: MD (22%)					
Voxels	*+ / -*	*Cluster peak*	*Other regions in cluster*	*MNI coordinates*	*Brodmann area*
200	-	R body of corpus callosum		-6, -18, 26	
155	+	fornix (column and body of fornix)		0, -14, 20	
87	+	unclassified	L body of corpus callosum	-24, -50, 4	
86	-	R corticospinal tract		4, -24, -36	
51	+	R frontal medial cortex		6, 42, -22	11
38	+	L parahippocampal gyrus, anterior division		-78	30
31	-	R lingual gyrus	R body of corpus callosum; R optic radiation	30, -44, -4	37
31	+	L lingual gyrus		0, -72, -2	unclassified
28	-	unclassified		-104	
27	-	L frontal medial cortex		-4, 48, -22	11

Cluster descriptions for C48

Modality: MO (30%)					
Voxels	*+ / -*	*Cluster peak*	*Other regions in cluster*	*MNI coordinates*	*Brodmann area*
42	+	R middle temporal gyrus, posterior division		52, -14, -20	20
40	+	L corticospinal tract		-62	
38	+	L precentral gyrus	L corticospinal tract	-10, -30, 62	4
38	-	L superior frontal gyrus		-16, 28, 38	32
38	+	R corticospinal tract		8, -28, -14	
36	-	L postcentral gyrus		-46, -16, 28	48
28	-	L middle frontal gyrus		-30, 16, 38	46
28	-	L middle frontal gyrus		-30, 15, 38	44
26	+	R lateral occipital cortex, superior division		22, -66, 36	7
25	+	L middle temporal gyrus, temporooccipital part		-48, -54, 0	37